J Neurophysiol 130: 1282–1302, 2023.
First published October 11, 2023; doi:10.1152/jn.00289.2023

american physiological society

JNP JOURNAL OF NEUROPHYSIOLOGY

RESEARCH ARTICLE

Control of Movement

Visual feature tuning properties of stimulus-driven saccadic inhibition in macaque monkeys

Fatemeh Khademi,[1,2] Tong Zhang,[1,2] Matthias P. Baumann,[1,2] Antimo Buonocore,[1,2,3] Tatiana Malevich,[1,2] Yue Yu,[1,2] and Ziad M. Hafed[1,2]

[1]*Werner Reichardt Centre for Integrative Neuroscience, Tübingen University, Tübingen, Germany;* [2]*Hertie Institute for Clinical Brain Research, Tübingen University, Tübingen, Germany; and* [3]*Department of Educational, Psychological and Communication Sciences, Suor Orsola Benincasa University, Naples, Italy*

Abstract

Saccadic inhibition refers to a short-latency transient cessation of saccade generation after visual sensory transients. This oculomotor phenomenon occurs with a latency that is consistent with a rapid influence of sensory responses, such as stimulus-induced visual bursts, on oculomotor control circuitry. However, the neural mechanisms underlying saccadic inhibition are not well understood. Here, we exploited the fact that macaque monkeys experience robust saccadic inhibition to test the hypothesis that inhibition time and strength exhibit systematic visual feature tuning properties to a multitude of visual feature dimensions commonly used in vision science. We measured saccades in three monkeys actively controlling their gaze on a target, and we presented visual onset events at random times. Across seven experiments, the visual onsets tested size, spatial frequency, contrast, orientation, motion direction, and motion speed dependencies of saccadic inhibition. We also investigated how inhibition might depend on the behavioral relevance of the appearing stimuli. We found that saccadic inhibition starts earlier, and is stronger, for large stimuli of low spatial frequencies and high contrasts. Moreover, saccadic inhibition timing depends on motion direction and orientation, with earlier inhibition systematically occurring for horizontally drifting vertical gratings. On the other hand, saccadic inhibition is stronger for faster motions and when the appearing stimuli are subsequently foveated. Besides documenting a range of feature tuning dimensions of saccadic inhibition to the properties of exogenous visual stimuli, our results establish macaque monkeys as an ideal model system for unraveling the neural mechanisms underlying a ubiquitous oculomotor phenomenon in visual neuroscience.

NEW & NOTEWORTHY Visual onsets dramatically reduce saccade generation likelihood with very short latencies. Such latencies suggest that stimulus-induced visual responses, normally jump-starting perceptual and scene analysis processes, can also directly impact the decision of whether to generate saccades or not, causing saccadic inhibition. Consistent with this, we found that changing the appearance of the visual onsets systematically alters the properties of saccadic inhibition. These results constrain neurally inspired models of coordination between saccade generation and exogenous sensory stimulation.

contrast sensitivity; motion; saccadic inhibition; spatial frequency; stimulus size

INTRODUCTION

Saccadic inhibition (1, 2) is an inevitable consequence of exogenous visual sensory stimulation (3). In this phenomenon, which also occurs for microsaccades (4, 5), the appearance of a visual stimulus, no matter how brief, is associated with an almost-complete cessation of saccade generation, and this cessation occurs with express latencies of <90–100 ms from stimulus onset (1, 2, 6–9). This conjunction of an early motor effect and a sensory origin driving it would suggest that saccadic inhibition reflects the arrival of visual sensory signals at the final oculomotor control circuitry relatively rapidly. Consistent with this, some studies in humans have demonstrated that saccadic inhibition (as observed with ongoing microsaccades during gaze fixation) depends on the contrast of the appearing visual stimuli (10–

Correspondence: Z. M. Hafed (ziad.m.hafed@cin.uni-tuebingen.de).
Submitted 30 July 2023 / Revised 3 October 2023 / Accepted 3 October 2023

12); this reinforces the notion that saccadic inhibition can reflect visual sensory feature tuning properties somewhere late in the visual-motor hierarchy (3). Moreover, stimulus size exhibits a modulatory effect on the latency and strength of saccadic inhibition for voluntary, target-directed saccades (7, 8). Exploiting the fact that saccadic inhibition and related smooth eye velocity modulations also occur during smooth pursuit eye movements (13–15) (for example, affecting catch-up saccades), yet other studies have shown a potential dependence on spatial frequency of the inhibitory oculomotor processes associated with saccadic inhibition (16).

Despite the fact that monkeys, constituting a highly suitable animal model for investigating neural mechanisms, also show robust saccadic inhibition, whether in controlled fixation tasks with microsaccades (5, 17, 18) or in free viewing paradigms (19, 20), the neural mechanisms driving saccadic inhibition remain elusive (3, 21). Earlier models have suggested that lateral inhibition in sensory-motor structures like the superior colliculus and frontal eye fields might play a role in this phenomenon (22–25). However, inactivation of neither the superior colliculus (26) nor the frontal eye fields (27) alters saccadic inhibition (for the case of microsaccades) in any meaningful way. Moreover, the detailed feature tuning properties of saccadic inhibition in monkeys have not yet been fully documented. We recently showed, again with microsaccades, that saccadic inhibition latency (and associated movement vector modulations) in macaque monkeys depends on the luminance polarity of the visual onsets (dark vs. bright contrasts) as well as on whether the onsets were of a small spot or of a large full-screen flash (28). This leaves a great deal more to desire: the use of monkeys to study the neural mechanisms underlying saccadic inhibition requires much further characterization of the visual feature tuning properties of this ubiquitous phenomenon in these animals.

In this article, we document a series of dependencies of saccadic inhibition in rhesus macaque monkeys on different visual feature dimensions. These feature dimensions include stimulus size, spatial frequency, contrast, orientation, motion direction, and motion speed. We also compare saccadic inhibition when different forms of gaze-orienting behaviors are triggered by the visual onsets. Experimentally, we exploited the fact that microsaccades continuously optimize eye position on the fixation spot (19, 29, 30); thus, they represent active oculomotor exploratory behavior on a miniature scale, which is fundamentally not different from free viewing (31). This is similar to human oculomotor behavior as well (32). Therefore, microsaccades represent an ideal experimental test bed for studying saccadic inhibition in general.

In what follows, we present evidence that the nature of the visual sensory signals present in the final oculomotor control circuits mediating saccadic inhibition can be quite distinct from the visual feature tuning properties of brain areas, such as early cortical visual areas, that might instead serve other aspects of scene analysis; the oculomotor system possesses its own filtered representation of the visual environment (33). These observations provide a solid foundation not only for exploring the neurophysiological mechanisms associated with saccadic inhibition in more detail but also for further future investigations of additional feature dimensions that might influence saccadic inhibition, such as color and form.

MATERIALS AND METHODS

Experimental Animals and Ethical Approvals

We collected data from three adult male rhesus macaque monkeys (*Macaca mulatta*) aged 7–14 yr and weighing 9.5–12.5 kg. All experiments were approved by ethics committees at the regional governmental offices of the city of Tübingen.

Laboratory Setup and Animal Procedures

The bulk of the data were collected in the same laboratory as that described in our earlier studies (34–36). Specifically, we used a CRT display spanning ~31° horizontally and 23° vertically. The display was ~72 cm in front of the animals, and it had a refresh rate of 85 or 120 Hz. The display was linearized and calibrated, and we used grayscale stimuli throughout the experiments. In some experiments in *monkeys A* and *F*, we used an LCD display with a refresh rate of 138 Hz (AOC AG273QX2700), which was also linearized and calibrated. Some of the behavioral tasks (e.g., dependence on the contrast of small, localized stimuli; see RESULTS) were obtained by reanalyzing behavioral data from an earlier study (34).

Data acquisition and stimulus control were realized through our custom-made system based on the Plexon-DATAPixx-Psychtoolbox system (PLDAPS) (37). The system connected a DATAPixx display control device (VPixx Technologies) with an OmniPlex neural data processor (Plexon) and the Psychophysics Toolbox (38–40).

The monkeys were prepared for the experiments previously, since they also contributed to several earlier publications by our laboratory; for example, see Refs. 34, 41. In the present purely behavioral experiments, we only measured eye movements by high-performance eye tracking. To do so, we exploited an implantation of a scleral search coil that we had previously done in one eye of each monkey, and we used the magnetic induction technique to track eye position (42, 43). Naturally, additional follow-up neurophysiological experiments in these animals will use the knowledge generated here to try to better understand the neural mechanisms underlying saccadic inhibition. Head position was comfortably stabilized during the experiments by attaching a small head-holder device implanted on the skull with a reference point on the monkey chair.

Experimental Procedures

In each experiment, the monkeys fixated a central fixation spot (square of ~5.4 × 5.4 min arc) presented over a gray background (of luminance 26.11 or 29.7 cd/m^2 for the CRT display and 36.5 cd/m^2 for the LCD display). The fixation spot was either black or white (depending on the experiment and date it was run), and it was only white in the experiment in which the subjects were instructed to generate a foveating saccade toward the appearing peripheral stimulus (see *experiment 5*). The luminance of the white fixation spot was 86 cd/m^2 in the CRT display and 132.5 cd/m^2 in the LCD display. After an initial period of fixation, typically lasting between 500 and 1,000 ms, a visual onset took place, which triggered saccadic inhibition.

Across different experiments, we varied the type of visual onset that took place, as we explain in more detail next.

Experiment 1: Size tuning.

During maintained fixation, a brief flash (~12- or ~7- to 8-ms duration) of a black circle centered on the fixation spot appeared. The circle had variable radius across trials from among eight possible values: 0.09° (approximately the size of the fixation spot being gazed toward), 0.18°, 0.36°, 0.72°, 1.14°, 2.28°, 4.56°, and 9.12° (approximately the size of the full display). Thus, we spanned a relatively large range of stimulus sizes.

Note that the brevity of the flash in this and some later experiments made it unlikely for a second saccadic inhibition event to take place in association with stimulus offset. That is, because of the integration windows of the visual system, the flash (rapid onset-offset event) acted more like a unitary stimulus transient causing a single saccadic inhibition occurrence. Slower display flicker will undoubtedly cause saccade rate oscillations (44), but we did not see evidence for this in our data.

We typically ran this experiment in daily blocks of ~200–500 trials per session, and we collected a total of 7,178, 9,078, and 3,103 trials in *monkeys A*, *F*, and *M*, respectively. This resulted in a total of 628–1,402 analyzed trials per condition per animal (after some exclusions, like when there were blinks around stimulus onset; see *Data Analysis*).

Experiment 2: Spatial frequency tuning.

In this set of experiments, we presented a vertical sine wave grating of high contrast (100%). The grating remained on until trial end a few hundred milliseconds later (300 ms). The monkeys were required to maintain fixation on the visible fixation spot. Across trials, the grating could have one of five different spatial frequencies as follows: 0.5, 1, 2, 4, and 8 cycles/° (cpd). The grating size was constrained by a square of 6° × 6° centered on the fixation spot. However, for some sessions in *monkey F*, the grating filled the entire display. The results were the same for the different grating sizes (since 6° × 6° was already relatively large), so we combined them in our analyses. The phase of the grating was randomized across trials.

We typically ran this experiment in daily blocks of ~150–400 trials per session, and we collected a total of 2,426 and 2,032 trials in *monkeys A* and *F*, respectively. This resulted in a total of 380–487 analyzed trials per condition per animal.

Experiment 3: Contrast sensitivity with full-screen stimuli.

In this set of experiments, the stimulus onset during active gaze fixation was a single display frame (~12 or ~7–8 ms) that was darker than the background (i.e., negative luminance polarity). This single-frame flash, which filled the entire display with a uniform luminance, could have the following contrast levels relative to the background (Weber contrast): 5%, 10%, 20%, 40%, and 80%.

We used negative luminance polarity in this and later experiments because it generally evokes stronger visual responses in the primary visual cortex than positive luminance polarity (45). Negative luminance polarity stimuli also evoke earlier visual responses in superior colliculus neurons (34), and they generally cause earlier saccadic inhibition (with full-screen stimuli) as well (46). Microsaccade direction modulations caused by localized peripheral stimuli are additionally stronger with negative luminance polarity stimuli (46). Nonetheless, we expect generally similar dependencies on features like contrast with positive luminance polarity stimuli.

We typically ran this experiment in daily blocks of ~200–600 trials per session. In total, we collected 4,623, 4,035, and 3,946 trials in *monkeys A*, *F*, and *M*, respectively. This resulted in a total of 760–1,321 analyzed trials per condition per animal.

Experiment 4: Contrast sensitivity with small, localized stimuli.

Here, we analyzed data from the fixation experiments of Ref. 34. That is, there was a stimulus onset during fixation consisting of a circle of 0.51° radius appearing somewhere on the display and staying on until trial end. The stimulus could have one of five different negative polarity (i.e., dark) Weber contrasts as follows: 5%, 10%, 20%, 50%, and 100%. We did not analyze the positive polarity (i.e., bright) contrasts from the previous study (34) because we wanted to compare saccadic inhibition to the task above with full-screen stimuli (but the results were expected to be generally similar).

We had a total of 3,854 and 8,551 analyzed trials from *monkeys A* and *M*, respectively, in this task. This resulted in 623–1,692 trials per condition per animal.

Experiment 5: Contrast sensitivity with small, localized stimuli and visually guided foveating movements toward them.

In this case, we used a task similar to that immediately above (*experiment 4*), except that we removed the fixation spot as soon as the peripheral stimulus appeared (34). This allowed the monkeys to generate a foveating saccade toward the appearing stimulus immediately after the saccadic inhibition that was triggered by the stimulus onset was completed. Our goal here was to compare the inhibition properties when the appearing stimulus was oriented toward with a foveating eye movement, as opposed to being completely ignored. That is, we tested what happens when the appearing stimulus (which was outside of the range of ongoing eye movement target locations when it occurred) was either ignored (*experiment 4*) or oriented toward (current experiment). The task was the same as the visually guided saccade task described in Ref. 34. It thus also contained randomly interleaved positive polarity stimuli, as in *experiment 4*.

We included a total of 1,928, 3,560, and 2,474 trials from *monkeys A*, *F*, and *M* in our analyses of this task. This resulted in ~52–915 trials per condition per animal in our analyses. Note that, in this experiment, not all contrasts were available as in *experiment 4*. Thus, the plots in RESULTS only show data from the contrasts that were actually tested.

Experiment 6: Motion direction and speed.

This experiment was similar to the spatial frequency tuning experiment above (*experiment 2*) but with a constrained stimulus size (6° × 6° centered on the fixation spot location). In the current case, the grating presented was a drifting grating having one of eight equally spaced motion directions and one of two temporal frequencies (4 or 16 Hz; equivalent to 3.64 and 14.55°/s motion speeds, respectively). The spatial frequency was constant across all trials: 1.1 cycles/°. At trial onset, the drifting grating appeared for 300 ms before the

monkeys were rewarded for keeping their gaze near the central fixation spot.

We included a total of 3,878, 1,218, and 6,327 trials from *monkeys A*, *F*, and *M* in our analyses of this task. This resulted in ~148–756 trials per motion direction (both speeds) per animal in the analyses.

Experiment 7: Orientation tuning.

Here, we tested whether a static oriented grating also influenced saccadic inhibition. In other words, because the drifting gratings of *experiment 6* above had both orientation and motion direction information simultaneously embedded within them, here we only explored the impact of orientation alone. The experiment was similar to *experiment 6*, except that we presented a full-screen stimulus onset consisting of a 2.12 cpd horizontal or vertical static grating of 100% contrast (and 1 of 2 possible phases). The grating remained on the display for a few hundred milliseconds (260–700 ms), and (as in other experiments) the fixation spot remained visible above the stimulus throughout the trial.

We ran this experiment on *monkeys A* and *M*. For *monkey M*, some of the trials not including any saccades were analyzed for our earlier documentation of ocular position drift responses with similar stimuli (46). However, the saccade data were not analyzed in either that previous study or any other study from our laboratory. For *monkey A*, we collected new data for the purposes of the present study. We analyzed a total of 1,338 and 1,352 accepted vertical and horizontal grating trials, respectively, from this monkey. From *monkey M*, we analyzed a total of 2,458 and 2,457 accepted vertical and horizontal grating trials, respectively. Note that the experiments also included an equal number of trials with oblique gratings (45° orientation). These trials, as expected, gave intermediate results between those of horizontal and vertical gratings (see RESULTS below), consistent with our observations from *experiment 6*. Therefore, we elected not to show the oblique orientation results for maximal clarity and simplicity.

Data Analysis

We detected all saccades with our established methods (47, 48). In all experiments, we included all saccades that happened in the peristimulus interval (regardless of their size), especially because we expected saccadic inhibition by stimulus onsets to affect all occurring movements in the monkeys (5). However, since the animals were engaged in fixation on a small target, the saccades were generally small anyway (e.g., median 18, 10, and 32 min arc in the prestimulus baseline fixation intervals of *experiment 6* in *monkeys A*, *F*, and *M*, respectively; similar values were observed in the other experiments).

In the orienting version of the contrast sensitivity task (*experiment 5*), we also detected the foveating saccade toward the appearing stimulus. This allowed us to limit the upper temporal boundary for analyzing the timing of saccadic inhibition (see below for how we estimated saccadic inhibition timing). In other words, once a foveating saccade is generated, no subsequent saccadic inhibition could occur because the foveating saccade can only proceed after the oculomotor system has already been reset (3).

We excluded trials if there were blinks in the peristimulus interval that we were interested in analyzing (from −500 ms to +1,000 ms relative to stimulus onset). Although some studies tape an additional wire loop on the eyelid of the animal to detect blinks with the same magnetic induction technique as for eye tracking (49), here we only used eye position measurements to detect blinks; that is, blinks are associated with characteristic eye movements that are easily detectable because of their speeds, amplitudes, durations, and directions (50), and this was sufficient to allow us to exclude unwanted epochs from analyses. We also excluded trials in which the monkeys broke their required gaze fixation state (either on the fixation spot or the foveated stimulus in the saccade task) before trial end. These were rare.

To compute saccade rate, we aggregated saccade onset times from all trials of a given condition and animal (we pooled data from the same condition across days of data collection in a given animal, but we always analyzed each monkey's data separately). We then created arrays that were 0 at all times except for the time samples of saccade onsets (assigned a value of 1; 1,000 Hz sampling rate). We then used a moving window of 50 ms, moving in steps of 1 ms, in which we counted the number of saccade onsets happening within the averaging window and within a given trial. This gave us a single rate estimate per trial. We then averaged across all trials to obtain the average saccade rate curve of the particular condition. Error bars around this average saccade rate were obtained based on the population of underlying single-trial rate estimates. For example, if there were 100 trials in a given condition, then each time sample of a rate curve had a population of 100 measurements, from which we could obtain both average rate as well as measures of confidence (such as 95% confidence intervals or standard errors of the mean). This approach is similar, in principle, to other standard saccade rate calculation approaches in the literature (12, 28). Subsequent analyses were made on the saccade rate curves that we obtained with this procedure.

Since saccadic inhibition happens very shortly after putative visual bursts in potential brain areas mediating the inhibition, we looked for hallmarks of feature tuning in the very initial phases of the stimulus-driven eye movement inhibition. To do this, we computed an estimate of the latency of the inhibition (called L_{50}), and we related this latency to the different stimulus properties. Figure 1*A* describes the conceptual idea of the L_{50} measure, which we defined as done previously in the literature (2, 12, 51). Briefly, we first measured baseline saccade rate in the final 100 ms of fixation before stimulus onset in any given condition. We did this by averaging saccade rate over this 100-ms period and pooling across all trials of the condition (e.g., for all trials with 0.5 cpd in *experiment 2*). We then estimated how much the rate dropped after stimulus onset during saccadic inhibition (i.e., the difference between the baseline rate and the minimum saccade rate after the stimulus onset). L_{50} was defined as the time point at which half of the rate drop during saccadic inhibition was achieved; the detailed robust estimate of this halfway drop is described exhaustively elsewhere (2, 12, 51). This measure is also conceptually similar to other estimates of saccadic inhibition timing (9), and we do acknowledge that other laboratories might elect to use alternative methods for estimating inhibition latency. We then repeated this procedure for all other conditions.

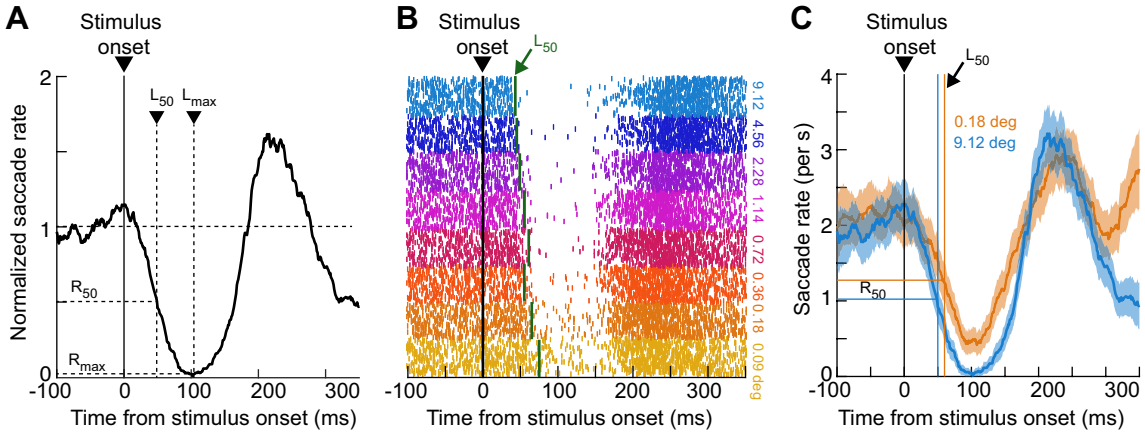

Figure 1. Relating saccadic inhibition to stimulus properties. *A*: example normalized saccade rate plot from 1 monkey and 1 condition. We were primarily interested in the time of saccadic inhibition, which we estimated via the L_{50} parameter described in the text; briefly, L_{50} indicates the time at which saccade rate dropped from baseline by half of the magnitude of its maximal drop caused by stimulus onset (L_{max}). We also report R_{50}, which is the raw saccade rate at the time of L_{50}. *B*: example relationship between L_{50}, saccadic inhibition, and stimulus properties from 1 animal and 1 experiment. The image shows all saccades occurring around stimulus onset that *monkey F* generated during *experiment 1* (size tuning). Each row represents a single trial's data, and each tick mark in a given row represents a saccade onset time within the given trial. The trials were grouped according to the size of the appearing stimulus (indicated by the color coding and associated key on *right*), and the vertical green lines indicate L_{50} estimates for each condition. As can be seen, L_{50} robustly indicated the timing of saccadic inhibition, which also clearly depended on stimulus appearance. Note that the large apparent density of tick marks per shown color is due to the fact that a large number of trials (~1,000) was collected per condition and not due to an unrealistically large saccade rate. *C*: example raw saccade rate from 1 monkey (*monkey A*) and 2 conditions of *experiment 1* (note that the blue curve shows the raw version of the same normalized data in *A*). Error bars denote 95% confidence intervals, obtained based on the population of available single-trial rate estimates. The *x*- and *y*-axis drop lines indicate the L_{50} and R_{50} values for each condition, respectively. As can be seen, saccadic inhibition timing reflected the change in stimulus property (in this case, size), also consistent with *B* in a second monkey. Figure 2 shows the full parametrization of size tuning of saccadic inhibition in all 3 monkeys.

Our L_{50} measure was a robust estimate of saccadic inhibition timing, as can be seen from Fig. 1*B*. This figure plots the raw saccade onset times of *experiment 1* from one example monkey (*monkey F*). The saccades are graphed as raster plots, with each row being a trial and each tick mark indicating saccade onset time relative to stimulus onset. Trials of the same type were grouped together and color-coded similarly for easier visualization (even though they were randomly interleaved during data collection). For each stimulus type, Fig. 1*B* also indicates the obtained estimate of L_{50}. As can be seen, this measure was a robust estimate of saccadic inhibition timing.

Even though L_{50} was our parameter of primary interest in this study (given the above text and Fig. 1*B*), we also sometimes reported R_{50}, which was simply the raw saccade rate (not normalized to the baseline rate) at which L_{50} was reached (Fig. 1*A*). This allowed us to document general variability of microsaccade rate (whether in baseline or at the L_{50} time of saccadic inhibition) across individual monkeys. The calculation of R_{50} was again based on previously published methods (12, 51).

Note also that we were not interested in postinhibition saccades (and how these saccades might depend on the visual stimulus properties). Postinhibition saccades reflect reprogrammed movements after the inhibition (3, 30, 52), and they depend on frontal cortical activity (27, 53, 54); we were, instead, interested in the immediate impact on eye movements as revealed by L_{50}. Nonetheless, for every experiment, we did plot example saccade rate curves that included the postinhibition movements as well, for completeness (e.g., Fig. 1*C*).

Table A1 in the APPENDIX provides descriptive statistics of L_{50} and R_{50} in all experiments and all animals, as well as estimates of baseline saccade rates in each animal and the total number of trials analyzed per condition. To obtain estimates of 95% confidence intervals for each measure of L_{50} and R_{50} in Table A1, we used bootstrapping. Briefly, if a condition had N trials, we randomly selected N trials (with replacement) in a given bootstrap, and we calculated L_{50} and R_{50}. We then repeated this process 1,000 times. The 95% confidence intervals were the intervals encompassing the range between the 2.5th and 97.5th percentiles of all of the 1,000 bootstrapped means. The obtained confidence intervals are also listed in Table A1.

When documenting the potential influence of a visual feature (e.g., contrast) on saccadic inhibition time (L_{50}), we also obtained the L_{50} measure for each condition and plotted it against the condition value (e.g., L_{50} vs. contrast). For the size tuning, spatial frequency, and contrast manipulations, we often noticed that L_{50} (and sometimes R_{50}) changed (either increased or decreased) with increasing stimulus size, spatial frequency, or contrast in an approximately logarithmic manner (see RESULTS). Thus, we obtained a fit to a function of the form $L_{50} = a \times \log_{10}(x) + b$, where x is the parameter being varied in an experiment (e.g., stimulus size or contrast) and a and b are the parameter fits. We include the fits in all relevant figures in RESULTS, with indications of r^2 values. We also used a similar approach for R_{50} plots, for completeness.

Similarly, when checking the dependence of saccadic inhibition on motion direction, we noticed that both L_{50} and prestimulus saccade directions exhibited clear directional anisotropies (see RESULTS). To quantitatively analyze these anisotropies and relate them to each other, we first normalized the dynamic range of either L_{50} or prestimulus saccade

count variations in any given direction. For example, if L_{50} was highest for upward motions and lowest for rightward motions, then we replotted L_{50} but now in the range from 0 to 1, with 1 being the normalized L_{50} value for upward motions and 0 being the normalized L_{50} value for rightward motions. We used a similar procedure when counting prestimulus saccades in any given direction; for example, if prestimulus saccades were most likely upward and least likely rightward, then we normalized saccade counts per direction bin such that the count in the upward bin was 1 and the count in the rightward bin was 0. We then fit each parameter (L_{50} or prestimulus saccade count in any given direction) to a sinusoidal function of the form $y(\theta) = a \cdot \cos(b \cdot \theta + c) + d$, where θ is the angular direction (of the motion patch for the L_{50} fit or of prestimulus saccades for the prestimulus saccade count fit) and a, b, c, and d are model fit parameters. We then compared how similar the frequency parameter (b) was for both L_{50} and prestimulus saccades. For the L_{50} fits, we binned θ into 8 directions, since this is what the experimental design gave us; for the prestimulus saccade fits, we binned prestimulus saccades into 16 equally spaced angular bins to give us a more robust visualization of the sinusoidal angular dependencies (see RESULTS).

RESULTS

We characterized the timing of saccadic inhibition (L_{50}; MATERIALS AND METHODS) as a function of visual stimulus properties across a series of feature manipulations in three different animals (Fig. 1). We were motivated by the hypothesis that saccadic inhibition reflects the impact of short-latency stimulus-driven visual bursts on final oculomotor pathways (3). If so, then feature changes that are expected to alter visual responses (somewhere in the brain that is relevant for the inhibition) should also alter the time of saccadic inhibition. For example, in Fig. 1*C*, two different stimulus sizes from *experiment 1* resulted in two different timings of saccadic inhibition in an example monkey. Therefore, we adopted a descriptive approach in this study, documenting our observations on saccadic inhibition in multiple feature dimensions.

Our efforts across all experiments described below motivate a search (in macaque monkeys) for neural loci in the final oculomotor control circuitry, possibly in the brain stem, that would exhibit stimulus-driven visual bursts of neural activity matching the feature tuning properties of saccadic inhibition that we document below. This would mean that early sensory areas (such as retina, lateral geniculate nucleus, and primary visual cortex) relay rapid visual signals to visually sensitive oculomotor areas, which might in turn reformat (33) these signals for specific use by the eye movement system, and for mediating the actual saccadic inhibition.

In the results below, besides saccadic inhibition timing (L_{50}), we also documented our measures of R_{50} (MATERIALS AND METHODS) because they roughly corresponded with the L_{50} modulations. Briefly, R_{50} describes the raw saccade rate at the L_{50} time. However, as stated above, we believe that the L_{50} modulations are the more meaningful ones, in general, since inhibition can be an all-or-none phenomenon in monkeys, especially for suprathreshold stimuli; this renders R_{50} closer to a floor effect for most stimulus features.

As also stated above, we additionally did not explicitly analyze postinhibition saccades (besides plotting saccade rate curves to include their time ranges). This was so because such postinhibition saccades reflect later processes (possibly also cognitively driven) (24, 55) that are needed to resume active oculomotor behavior after stimulus-driven interruption (also see the results of *experiment 5* below). Indeed, prior work has shown that these postinhibition saccades may be governed by underlying neural processes different from those generating the more reflexive phenomenon of saccadic inhibition (27, 30, 52–54).

Larger Stimuli Cause Earlier Saccadic Inhibition

In our first experiment, we briefly presented a black circle centered on the fixation spot (MATERIALS AND METHODS). Across trials, the circle could have one of eight different radii, ranging from 0.09° (approximately the size of the fixation spot) to 9.12° (approximately filling the whole display). We found that saccadic inhibition times roughly monotonically decreased with increasing stimulus size, as demonstrated in Fig. 2. This figure is organized as follows. For each animal (Fig. 2*A* for *monkey A*, Fig. 2*D* for *monkey F*, and Fig. 2*G* for *monkey M*), we first show the saccade rate modulation time courses as computed in Fig. 1, *A* and *C*. Here, each curve represents a different stimulus size that was presented. As can be seen, saccadic inhibition started earlier for larger onset sizes, and the dependence on size was roughly logarithmic. Specifically, Fig. 2, *B*, *E*, and *H*, show measures of L_{50} (our estimate of saccadic inhibition time; Fig. 1 and MATERIALS AND METHODS) as a function of stimulus radius, using a logarithmic x-axis. In all three animals, the data roughly followed a straight line of negative slope (goodness of fits to a logarithmic curve are indicated in the respective figure panels). Thus, with a flash as little as 1–2° in radius, saccadic inhibition was already stronger than for even smaller visual transients, and the effect eventually approached a plateau with even larger stimuli.

The results for R_{50} (the actual raw saccade rates at the time of L_{50}; MATERIALS AND METHODS) mimicked the above observations of L_{50}, as can be seen from Fig. 2, *C*, *F*, and *I*. This is consistent with human observations (7, 8). Note, however, that L_{50} may be the more sensitive measure of stimulus-dependent changes in saccadic inhibition since saccade rate drops to almost zero (i.e., hits a floor effect) for most stimulus sizes (e.g., Fig. 2, *A*, *D*, and *G*). This is why our primary focus in this article, in general, was to document the L_{50} effects.

Thus, in rhesus macaque monkeys, saccadic inhibition shows a clear dependence on visual transient size, providing a clear homolog of human results with saccades in a different context (7, 8). This motivates the use of macaque monkeys to study the neurophysiological mechanisms underlying saccadic inhibition.

High Spatial Frequencies Are Associated with Delayed Saccadic Inhibition

We next turned our attention, in a second experiment, to the influences of spatial frequency on saccadic inhibition in rhesus macaque monkeys. Here, the monkeys fixated a central fixation spot while we presented a vertical sine wave

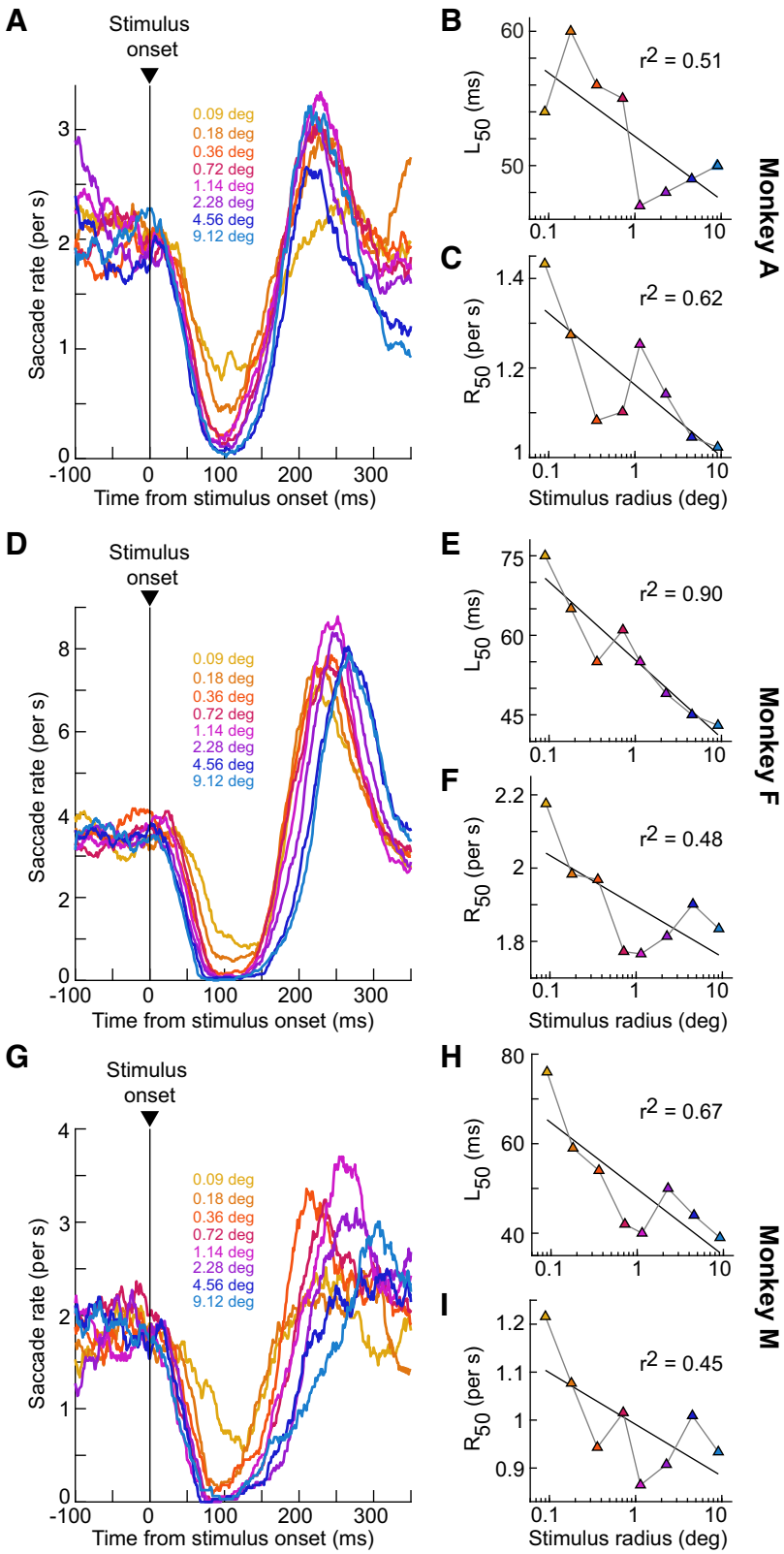

Figure 2. Earlier saccadic inhibition with larger stimuli (*experiment 1*). *A*: raw saccade rate curves relative to stimulus onset (as in Fig. 1) from *monkey A* in our size tuning experiment. Each colored curve corresponds to a stimulus radius as per the color-coded key. Larger stimuli were associated with earlier and stronger saccadic inhibition. *B*: a measure of saccadic inhibition time (L_{50}) as a function of stimulus radius (MATERIALS AND METHODS). Saccadic inhibition started earlier with larger stimuli, and the effect followed a roughly logarithmic relationship: the black line describes the fit to a logarithmic function (MATERIALS AND METHODS) with the r^2 value shown. *C*: similar to *B* but for a measure of saccadic inhibition strength (R_{50}; MATERIALS AND METHODS). Again, there was a stronger inhibition with larger stimulus sizes. *D–F*: similar observations from *monkey F*. *G–I*: similar observations from *monkey M*.

grating of variable spatial frequency across trials. The grating stayed on the display until the monkeys were rewarded 300 ms later, and in some cases it filled the whole display (MATERIALS AND METHODS). Figure 3*A* shows the saccade rate curves of *monkey A* in this experiment. The monkey's saccadic inhibition was systematically delayed with increasing spatial frequency of the appearing stimuli. This dependence was again roughly logarithmic, as can be seen from Fig. 3*B*

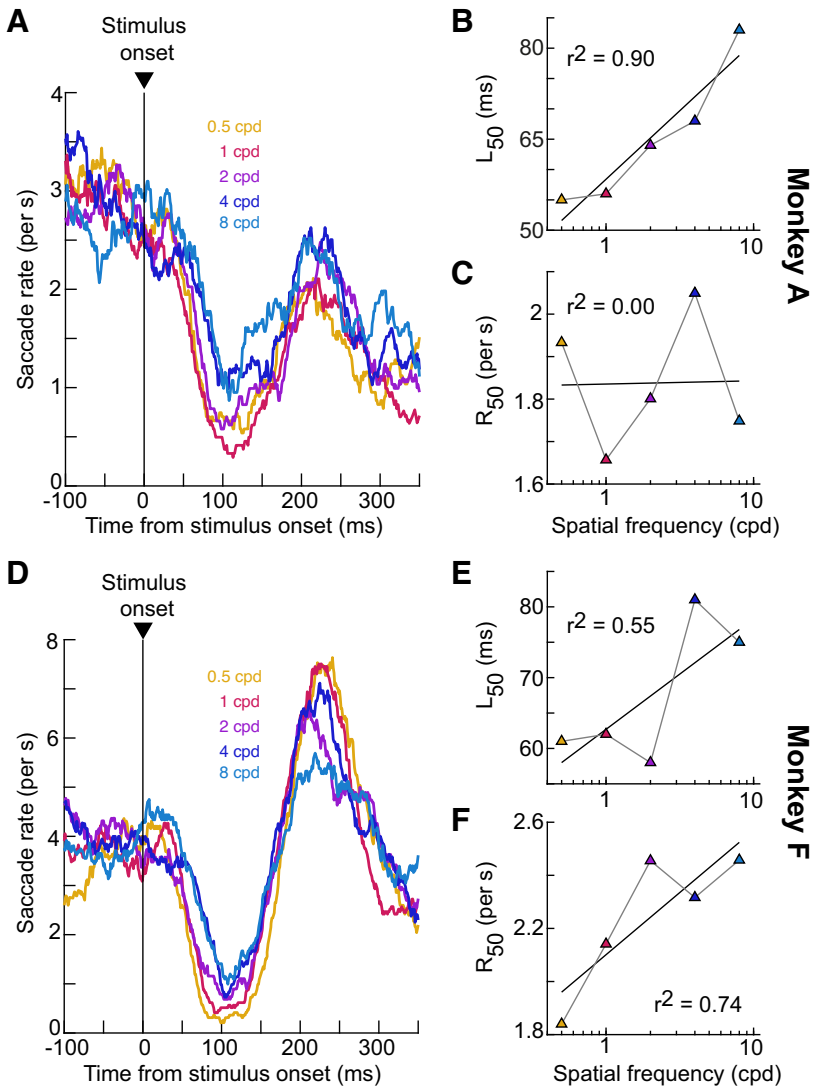

Figure 3. Earlier saccadic inhibition with lower-spatial frequency stimuli (*experiment 2*). *A*: raw saccade rate curves from *monkey A* in the spatial frequency tuning experiment. Each curve now reflects saccade rate modulations for a stimulus onset of a given spatial frequency (indicated by the color-coded key). There was earlier and stronger saccadic inhibition for the low-spatial frequency stimulus onsets. *B*: inhibition time (L_{50}) as a function of spatial frequency. This figure is formatted similarly to Fig. 2, *B*, *E*, and *H*. Inhibition time increased with a roughly logarithmic dependence as a function of increasing spatial frequency; the black line describes the best-fitting logarithmic function equation (same as in Fig. 2) to the data (MATERIALS AND METHODS). *C*: inhibition magnitude as assessed with R_{50} for the same data. Here, there was no clear relationship between R_{50} and spatial frequency (see text). *D–F*: similar analyses *for monkey F*. In this case, not only L_{50} but also R_{50} increased with stimulus spatial frequency.

and the associated logarithmic function fit (MATERIALS AND METHODS). L_{50} in this animal was ~55 ms for 0.5 cpd gratings, but it was almost 85 ms for 8 cpd gratings. In this monkey, R_{50} did not systematically change as a function of spatial frequency (Fig. 3*C*). This is likely because the monkey's prestimulus saccade rate was time varying (continuously decreasing) as a result of the animal gradually reducing its baseline saccade rate in anticipation of trial end; this time-varying baseline added variability to our R_{50} measures.

In the second monkey that we tested with this task (*monkey F*), very similar observations were made for L_{50}: the time of saccadic inhibition increased with increasing spatial frequency (Fig. 3, *D* and *E*). Since this monkey's baseline (prestimulus) saccade rate was more constant than in *monkey A*, and also since the monkey's minimum saccade rate during inhibition was markedly different from the baseline rate (Fig. 3*D*), the R_{50} measure also showed an increasing dependence on spatial frequency like for L_{50}. Since R_{50} reflects the dynamic range of saccadic inhibition strength (MATERIALS AND METHODS), this means that in addition to being later saccadic inhibition was also weaker with higher spatial frequencies (minimum saccade rate during inhibition was higher).

Thus, saccadic inhibition in rhesus macaque monkeys shows a low-pass spatial frequency tuning characteristic. It is interesting that visual processing in the oculomotor system also exhibits low-pass spatial frequency tuning properties (56, 57). This might suggest that as signals proceed from the retina and through the early visual system, the relevant visual response characteristics that might ultimately shape the feature tuning properties of saccadic inhibition can be different from the characteristics of early visual areas like primary visual cortex (which exhibits more band-pass spatial frequency tuning).

Earlier Saccadic Inhibition with Higher Contrasts

Since previous human experiments demonstrated a dependence of saccadic inhibition on stimulus contrast (10–12), our next set of manipulations focused on this visual feature. The first such manipulation involved the onset of a full-screen flash of variable contrast across trials. The flash was of negative luminance polarity (darker than the

background), and it occurred at a random time during fixation (MATERIALS AND METHODS). In all three monkeys tested with this task, saccadic inhibition clearly occurred earlier for higher contrasts than for lower ones (Fig. 4, *A*, *D*, and *G*). Moreover, the time of L_{50} was again approximately logarithmically related to contrast level (Fig. 4, *B*, *E*, and *H*). Thus, consistent with humans, rhesus macaque monkeys show a dependence of saccadic inhibition timing on stimulus contrast. Our measures of R_{50} also behaved similarly to L_{50} (Fig. 4, *C*, *F*, and *I*), suggesting a larger drop in saccade likelihood at the time of peak saccadic inhibition for high-contrast stimuli.

We next ran another experiment in which stimulus contrast was again manipulated. However, in this case, the stimulus onset consisted of a small disk of radius 0.51° (34). This disk appeared on the display and remained on for a few hundred milliseconds, but it was to be ignored by the monkeys. The location of the disk varied from session to session, especially because the data from this experiment came from a previous neurophysiological study in which we were also recording superior colliculus visual neural activity (34). Here, we analyzed the negative luminance polarity conditions from that study (to behaviorally match them with the experiment of Fig. 4 using dark contrasts). As can be seen from Fig. 5, even with small, localized stimuli L_{50} still decreased with increasing stimulus contrast, consistent with the results of Fig. 4.

The R_{50} effects were noisier in Fig. 5, only showing a more convincing negative trend for *monkey A*. This could be because the saccadic inhibition effect was overall weaker in this experiment than in the experiment of Fig. 4. For example, at 100% contrast, the minimum saccade rate in *monkeys A*, *F*, and *M* was 0.15, 0, and 0.33 saccades/s, respectively, in Fig. 4; it was 1.4 and 1.47 saccades/s in *monkeys A* and *M*, respectively, in Fig. 5. Thus, in Fig. 5 the minimum saccade rate that was reached during peak saccadic inhibition was higher than that in Fig. 4, an observation that is at least partially due to the smaller stimulus sizes (Figs. 1 and 2). That being said, stimulus size alone was not the full explanation for the difference. In fact, a similar stimulus size presented in the fovea (that is, aligned with the goal locations of the saccades; Fig. 2) caused stronger peak inhibition than in Fig. 5 with peripheral stimulus presentations. This suggests that stimulus onset locations relative to either the fovea or the instantaneous goal of saccades can modulate the strength of saccadic inhibition. In any case, the difference in saccadic inhibition strength across the experiments of Figs. 4 and 5 led us to next ask what happens if the stimulus onset was to be foveated as opposed to being completely ignored.

Stronger Saccadic Inhibition When Appearing Stimuli Are Targets for Foveation

The results of Figs. 4 and 5 demonstrate that saccadic inhibition depends on stimulus contrast in general but that an ignored small stimulus away from the oculomotor targets of the ongoing saccadic activity may be associated with generally weaker peak inhibition than a larger visual transient spanning the retinotopic target locations of the ensuing saccades (since the transient covered the fixation spot). That is, at the time of peak saccadic inhibition, there was still a higher likelihood of saccade occurrence with the ignored eccentric stimulus (Fig. 5) than with a large visual transient covering the perifovea (where our small saccades were targeted in our gaze fixation tasks) (Fig. 4). However, if the eccentric stimulus is now to be foveated, then the interruption by the visual onset (3) should eventually lead to a foveating eye movement toward the stimulus. In this case, postinhibition saccades are much more cognitively controlled; they are targeted eye movements toward the appearing stimuli. We found that in this case saccadic inhibition became all or none. Specifically, we repeated the same experiment of Fig. 5, but now requiring the monkeys to foveate the appearing stimulus. As stated in MATERIALS AND METHODS, this experiment had stimulus conditions and timings similar to *experiment 4*, except that the fixation spot was removed simultaneously with eccentric target onset.

Saccadic inhibition as caused by a visual onset in this new foveating eye movement experiment generally followed a timeline similar to saccadic inhibition when the appearing stimulus was completely ignored in the previous experiment. For example, Fig. 6, *A*, *C*, and *E*, show the saccade rate curves around stimulus onset from the 100% contrast condition in the two cases. The black rate curves replicate the 100% contrast data from Fig. 5, and they are included in Fig. 6 only up to the peak inhibition time. The blue rate curves instead show saccade rate when the task was to foveate the appearing target after the stimulus-driven saccadic inhibition had begun. In this case, we plotted the rate curves until the time of the foveating saccade that had the lowest reaction time from stimulus onset. Note also that *monkey F* only performed the foveating saccade version of the task, so we did not show any black curve in this monkey's panel. As can be seen, in all three animals, when the goal was to foveate the appearing eccentric stimulus, saccadic inhibition was an all-or-none phenomenon (that is, saccade rate dropped to 0). Although it is true that the baseline (prestimulus) saccade rate was different in the two tasks, peak saccadic inhibition in Fig. 5 never caused zero saccade rates during the inhibition period, even at high contrast (the black curves in Fig. 6 are truncated at the minimum saccade rate and were always well above 0). Consistent with this, across all contrasts, the R_{50} measure in all three animals was lower than the same measure from the very similar task of Fig. 5. This comparison between the two tasks is rendered easier in Fig. 6, *B*, *D*, and *F*, plotting R_{50} from the data of Fig. 5 in the same panels as R_{50} from this additional experiment (again, *monkey F* was not tested in the fixation version of the task, so only the current experiment's results are shown; also, *monkey M* was not tested with all contrasts in this experiment, so only the tested data points are shown). R_{50} was lower in the current experiment than in the previous one.

Therefore, saccadic inhibition can have generally similar time courses depending on the subsequent postinhibition oculomotor behavior (Fig. 6, *A*, *C*, and *E*), but the peak inhibition strongly depends on such behavior. Naturally, in this version of the task the fixation spot was also extinguished at the same time as when the eccentric stimulus appeared. Since the active oculomotor behavior was generally aimed at the fixation spot (19, 29, 30), it could be that we obtained stronger saccadic inhibition in this case because there was a double visual transient (a peripheral target onset as well as a simultaneous foveal target offset). Nonetheless, these data

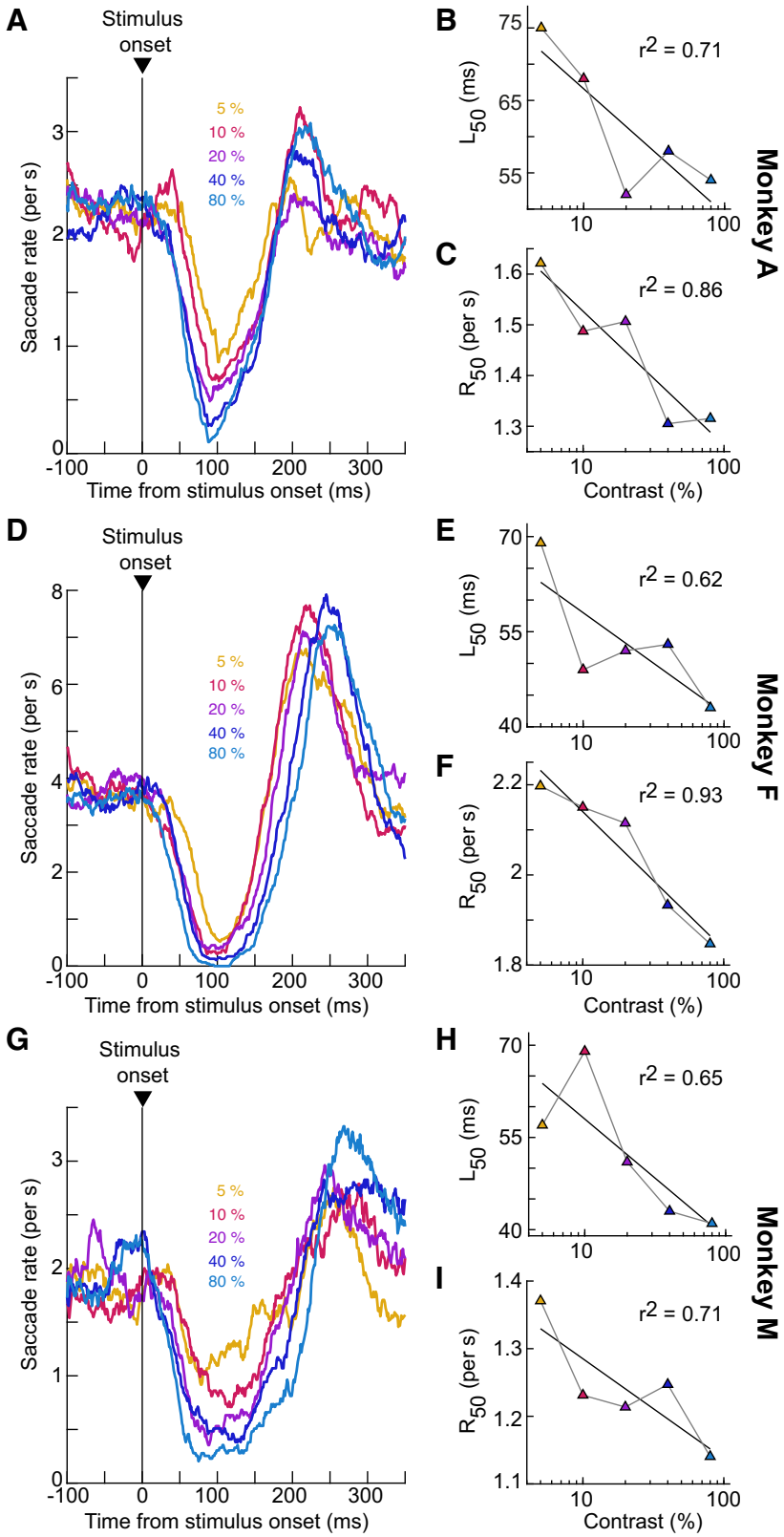

Figure 4. Earlier saccadic inhibition with higher contrasts of large stimuli (*experiment 3*). *A–C*: analyses similar to those in Figs. 2 and 3, but now relating saccadic inhibition in *monkey A* to the contrast of a full-screen flash appearing. Both saccadic inhibition time (L_{50}) and strength (R_{50}) were contrast dependent: L_{50} decreased with increasing contrast, and inhibition strength increased with increasing contrast (evidenced by reduced R_{50} rates). *D–F*: similar observations for *monkey F*. *G–I*: similar observations for *monkey M*. Note that *A*, *D*, and *G* show raw (not normalized) saccade rates.

touch on an interesting question about how multiple different orienting behaviors can be coordinated around the time of stimulus onsets, and they can inform neurophysiological studies of both saccade generation and fixation maintenance in the face of asynchronous external inputs (3). This idea also extends to expected direction modulations in microsaccades after stimulus onsets (4, 58). Indeed, it is interesting to note that we previously found similar microsaccade direction

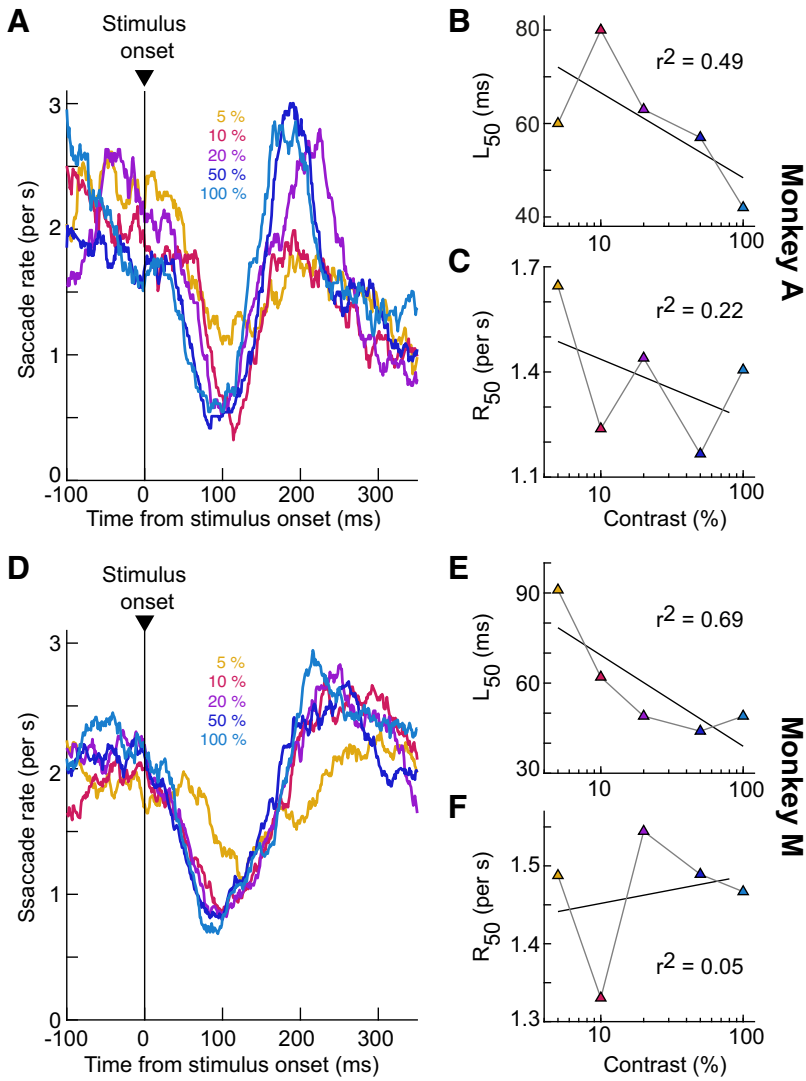

Figure 5. Earlier saccadic inhibition with higher contrasts of small, localized stimuli away from the oculomotor goals of ongoing saccades (*experiment 4*). *A–C*: analyses similar to Fig. 4. but now with the stimulus being a small disk (radius 0.51°) appearing somewhere on the display away from where the ongoing saccades were being generated. Saccadic inhibition time (L_{50}) still decreased with increasing contrast. The rate effect (R_{50}) was less clear as in Fig. 4, likely because the stimulus onset was actively ignored (also see Fig. 6 for additional evidence). *D–F*: similar observations from *monkey M*. Here, the rate effect was even weaker than in *monkey A* (also see Fig. 6). Again, *A* and *D* show raw rather than normalized saccade rates.

modulations after a peripheral stimulus onset when the stimulus was to be either foveated or not (Ref. 30, e.g., see their Fig. 4).

Dependence of Saccadic Inhibition on Motion Direction and Image Orientation

In our next experiment, the stimulus onset consisted of a drifting grating possessing one of eight possible motion directions and one of two possible temporal frequencies. We first analyzed the influence of motion direction on saccadic inhibition, by pooling across temporal frequencies. Figure 7*A* shows example saccade rate curves around the time of the onset of the drifting gratings. Figure 7*A*, *top*, shows saccade rate from *monkey A* when the grating was drifting upward, and Fig. 7*A*, *middle*, shows saccade rate when the grating was drifting leftward. Figure 7*A*, *bottom*, describes saccade rate with downward drifting gratings (data for the rightward motion direction are summarized below and in Fig. 7*B*). In all cases, the location of the stimulus was the same; only the motion direction of the gratings was different across panels. Saccadic inhibition occurred earlier for the leftward motion direction than for both vertical motion directions (vertical: colored lines indicate L_{50} for each case). Figure 7, *D* and *G*, show similar observations across the other two monkeys.

Interestingly, when we tested all motion directions in each animal (Fig. 7, *B*, *E* and *H*), we found slightly variable dependencies of the time of saccadic inhibition on motion direction in each individual. Specifically, although it was generally true that horizontal motion directions were associated with earlier L_{50} times than vertical ones (Fig. 7, *A*, *D* and *G*), each monkey showed a specific set of additional motion directions with particularly long L_{50} times relative to the others. In *monkey A*, this was the case for upward-leftward motion directions; in *monkey F*, this was the case for upward-rightward motion directions; and in *monkey M*, this was the case for upward or downward motion directions.

We next considered a potential correlate of such individual monkey idiosyncrasy. Specifically, we analyzed the direction distribution of microsaccades in each monkey during baseline fixation, before any stimulus appeared. To do this, we picked an interval before stimulus onset (final 100 ms before the onset event occurred) across all motion directions. We then plotted the angular distribution of saccade

directions in this baseline interval. The saccade direction distributions of all three animals are shown in Fig. 7, *C*, *F*, and *I*. As can be seen, the dependence of L_{50} in each animal was correlated with the animal's intrinsic saccade direction distribution during baseline intervals. For example, *monkey A* tended to make more up-left oblique saccades, whereas *monkey F* tended to make more up-right oblique movements. In both cases, L_{50} was longer in a corresponding direction for the respective animal. Similarly, *monkey M* made more frequent vertical saccades than horizontal saccades (Fig. 7*I*), and this again was correlated with longer L_{50} times for vertical motion directions.

To better quantify this potential relationship between L_{50} modulations for the different motion directions and prestimulus baseline saccade direction anisotropies, we plotted L_{50} values (after normalization) as a function of stimulus motion direction for each monkey (green in Fig. 8). Given the results of Fig. 7, this resulted in a sinusoidal relationship between L_{50} and motion direction in each animal (as also evidenced by the fitted sinusoidal curves; MATERIALS AND METHODS). We then plotted, on the same graphs (red in Fig. 8), the likelihood of prestimulus baseline saccades as a function of all possible saccade directions that could occur (again after normalizing the saccade direction distributions; see MATERIALS AND METHODS for details). In each monkey, it was interesting to see that both the frequency and the phase of the fitted sinusoids were similar whether we were characterizing the L_{50} direction dependencies or the prestimulus saccade direction anisotropies. This similarity was also evident in the underlying raw data themselves (dots with connecting lines in Fig. 8). Thus, there was a relationship between the L_{50} modulations as a function of motion direction and the underlying prestimulus baseline saccade direction idiosyncrasies of each animal. We also, naturally, confirmed that the prestimulus saccade direction anisotropies in Fig. 8 were still present in other tasks not involving moving stimuli (such as the size tuning task above).

These observations might suggest that each monkey experiences more frequent retinotopic motion directions during self-movement because of the intrinsic biases in saccade directions. It could, therefore, be that saccadic inhibition is easier for the more frequently experienced retinal motion directions. This would be interesting to investigate in more detail in the future.

It is also interesting that horizontal motions were generally easier to inhibit (shorter L_{50} times) than vertical motions. This could reflect stronger visual signals for horizontal motion directions, and it could fit with a relatively large literature showing how vision in the horizontal cardinal dimension might be better than vision in the vertical cardinal dimension (59–61). That being said, an additional contributing factor to the results of Figs. 7 and 8 could be the grating orientation itself. That is, horizontal motions in Fig. 7 involved presenting a vertical drifting grating, and vertical

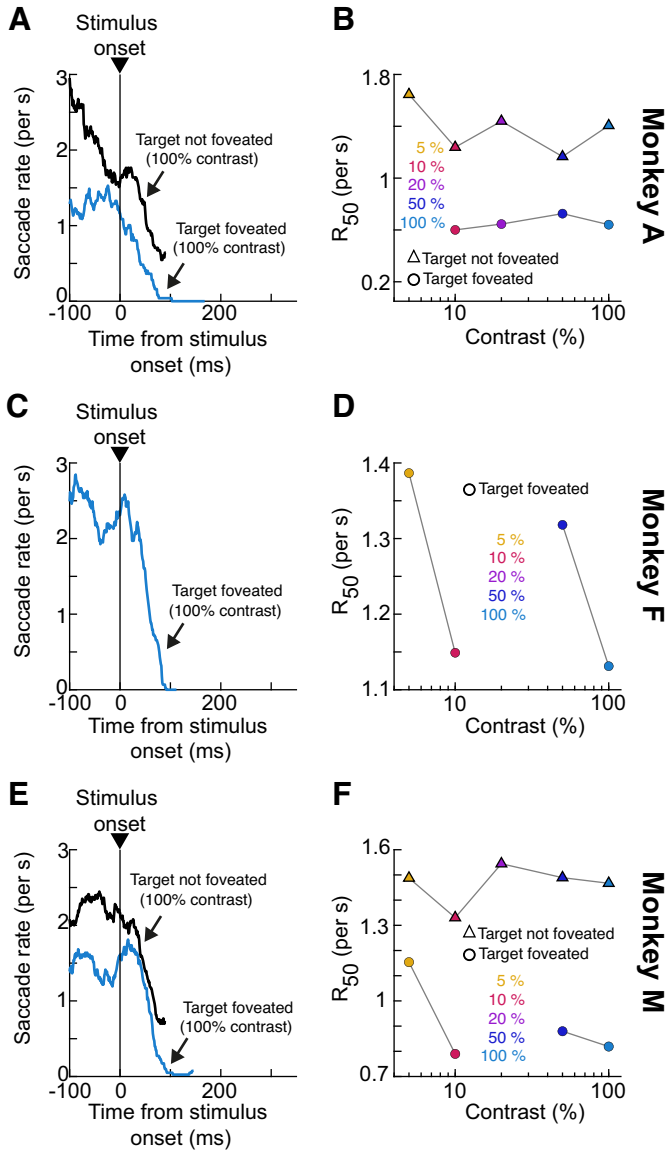

Figure 6. Stronger saccadic inhibition when the appearing stimuli were to be later foveated (*experiment 5*). *A*: the black curve shows the same raw saccade rate curve as that from Fig. 5 for 100% contrast stimuli in *monkey A*. The blue curve shows the raw saccade rate curve for the same stimulus and monkey, but now when the stimulus was to be subsequently foveated with a targeting eye movement (*experiment 5*). The black curve is truncated at the point of maximum saccadic inhibition, and the blue curve is truncated at the time of the shortest-latency foveating saccade. Saccadic inhibition started at approximately the same time in both cases (the black curve had a time-varying prestimulus saccade rate in this monkey, as we also saw in Fig. 3*A*; this monkey tended to perform fixation tasks by gradually decreasing saccade rate in anticipation of stimulus onset and trial end). However, saccadic inhibition was all or none when a subsequent foveating saccade was made. *B*: consistent with this, across all tested contrasts in both experiments, saccadic inhibition strength (R_{50}) was lower in the foveated target condition. Note that the data for the condition without foveating saccades shown here is the same as that in Fig. 5*C* (included here for easier comparison to the other curve). *C* and *D*: similar analyses for *monkey F*. This monkey did not perform the experiment of Fig. 5, but the data from the current experiment still show all-or-none saccadic inhibition, consistent with *monkey A*. This monkey would have also shown consistent results in Fig. 5 with the other 2 monkeys. For example, like the other 2 monkeys, this monkey's prestimulus saccade rate in the current experiment was lower than in experiments not requiring a foveating saccade (e.g., compare to Figs. 3 and 4). *E* and *F*: similar analyses for *monkey M*. Here, both variants of the task were collected, and the same results as with *monkey A* can be seen. That is, inhibition time was similar in both task variants; however, when the appearing target was later foveated, saccadic inhibition magnitude was much stronger (smaller R_{50}).

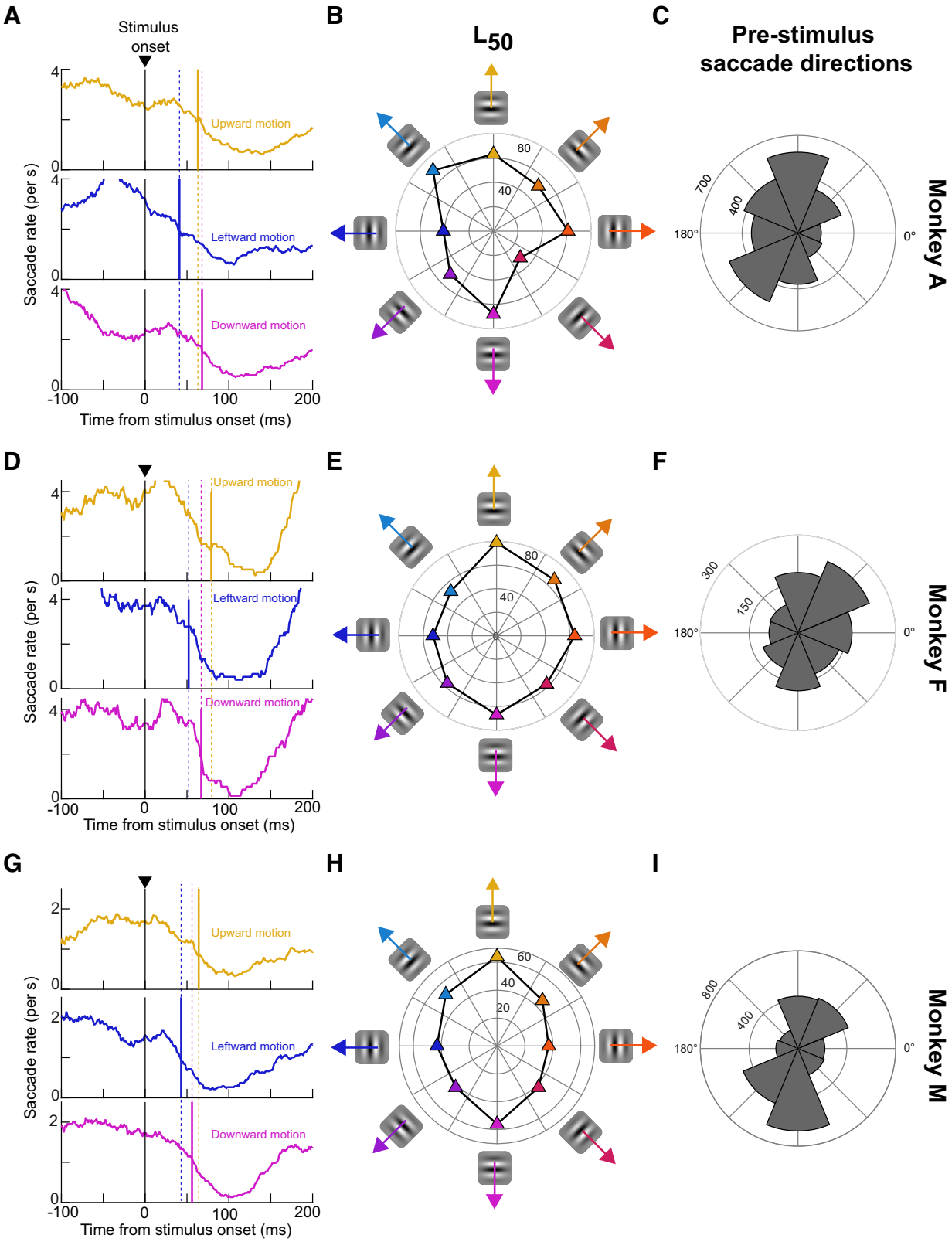

motions involved presenting a horizontal drifting grating. Given that, for example, upward versus downward motion directions gave rise to similar L_{50} times in general, it could be that the driving factor for the observed L_{50} times was the shared grating orientation between these two conditions. Thus, our final experiment in this study involved presenting static oriented gratings. Consistent with the results in Figs. 7 and 8, we found that vertical static gratings were indeed

associated with earlier saccadic inhibition than horizontal gratings in both monkeys that we tested in this experiment (Fig. 9). Thus, both motion direction (compare rightward vs. leftward motions in Fig. 7, *B*, *E*, and *H*, giving rise to slightly different L_{50} times) and orientation (compare horizontal vs. vertical static gratings in Fig. 9) influence the timing of saccadic inhibition.

Dependence of Saccadic Inhibition on Motion Speed

Finally, we pooled across all motion directions from Fig. 7 to check whether there was an impact of motion speed on saccadic inhibition. We had two motion speeds in the drifting gratings, characterized by two different temporal frequencies. We found that saccadic inhibition timing in all three monkeys generally did not strongly depend on motion speed (Fig. 10; colored L_{50} lines). However, faster speeds caused a deeper and longer-lasting minimum of saccade rate than slower speeds in all three animals (Fig. 10). Thus, recovery from saccadic inhibition was harder for the faster motion speeds in all three monkeys.

DISCUSSION

We characterized the properties of saccadic inhibition in rhesus macaque monkeys as a function of different visual feature dimensions. We found that saccadic inhibition in these animals systematically depends on stimulus size, spatial frequency, contrast, orientation, and motion direction. We also found that if appearing stimuli are subsequently foveated as opposed to being ignored, saccadic inhibition is stronger and becomes much more like an all-or-none phenomenon. On the other hand, relatively small eccentric "distractors" that are ignored have significantly milder inhibitory effects on saccade generation.

Some of the feature dimensions that we tested, like stimulus contrast, were also tested previously in humans and with microsaccades (10–12). The similarity of our findings in monkeys to those observations in humans reinforces our belief that macaque monkeys are a suitable model system for exploring the neural mechanisms of saccadic inhibition. In fact, recent transcranial magnetic stimulation (TMS) studies of the human homolog of the monkey frontal eye fields also affirm the utility of monkeys for investigating neural mechanisms of phenomena related to microsaccadic inhibition (53, 54). Specifically, these TMS studies disrupted postinhibition saccades with disruption of frontal eye field activity, consistent with the predictions from reversible inactivation of the frontal eye fields of macaque monkeys (27). This homology between the two species is exactly why we performed the present experiments. These experiments provide, in our view, a reference frame with which we hope to inform our upcoming neurophysiological studies of saccadic inhibition in the near future.

We think that we are likely to see future neurophysiological experiments revealing an important role for oculomotor control circuits in the midbrain and brain stem in mediating saccadic inhibition. Indeed, visual responses in the superior colliculus already hint that such responses in oculomotor control circuitry can matter a great deal for saccade generation. For example, collicular visual responses occur earlier for low- rather than high-spatial frequency stimuli, and this mimics the patterns of saccadic reaction times in visually guided saccade paradigms (56). Similarly, express saccades (saccades with reaction times less than ~90–100 ms) seem to be triggered by direct readout of the spatial locus of superior colliculus visual bursts (occurring within 50–100 ms from stimulus onset) (62). Thus, in the case of express saccades, visual sensory responses do indeed have a direct impact on saccade generation. Likewise, we think that visual responses in the oculomotor control network should have a direct impact on saccadic inhibition, again because of the very short latency with which inhibition is achieved. In this case, we might predict (3, 21) that such an impact of visual responses should be inhibitory (rather than excitatory as in the case of the superior colliculus and express saccades). Such an inhibitory effect could arise if omnipause neurons in the brain stem (63–65) exhibited visual pattern responses to stimulus onsets of different feature properties, and if these responses were consistent with the feature tunings that we discovered in the present study.

The above thoughts lead to the idea that the scene analysis that takes place by oculomotor control circuits in the brain, via the sensitivity of these circuits to visual inputs, is a reformatted representation of the scene. That is, it may not be needed for the superior colliculus and other oculomotor control circuits to just inherit the visual properties of the primary visual cortex or other cortical areas, even if the signals eventually come from these cortical areas. Rather, the representation is reformatted for something useful for the oculomotor system (33). This is not unlike evidence that the superior colliculus seems to favor the upper visual field (66, 67) when ventral stream visual cortical areas might favor the lower visual field (68). Thus, the oculomotor system "sees" a filtered representation of the visual scene that is not necessarily the same as what cortical areas for scene analysis and interpretation might "see," and this is still the case even if it is the signals in the early cortical visual areas (like primary visual cortex) that are ultimately relayed to the oculomotor control network.

If that is indeed the case, then one question that might arise in relation to our results in the present article could be,

Figure 7. Later saccadic inhibition for vertical motion directions (*experiment 6*). *A*: raw saccade rate curves of *monkey A* from 3 example motion directions in *experiment 6*. Each curve is truncated vertically and horizontally to focus on the saccadic inhibition phase. The vertical colored lines indicate saccadic inhibition time (L_{50}) for their respective saccade rate curves. As can be seen, saccadic inhibition occurred earlier for leftward motion directions than for both upward and downward motion directions. *B*: values of L_{50} in this experiment and animal for all tested motion directions. Horizontal motions generally had shorter L_{50} values than vertical directions. Up-left motion directions also had the longest L_{50} values. *C*: we plotted the angular distribution of saccade directions during a prestimulus baseline interval and noticed that the biases in *B* could be correlated with those in the current panel. For example, the monkey made more saccades in the upward and leftward direction, and up-left motions were associated with delayed saccadic inhibition. *D–F*: similar observations in *monkey F*. Again, horizontal motion directions were associated with smaller L_{50} values than vertical motion directions. Moreover, in this case, L_{50} was additionally longer in the up-right than in the up-left motion direction (*E*), and this was correlated with the monkey's intrinsic bias to make more baseline saccades toward the upper right direction (*F*). *G–I*: similar observations in *monkey M*. Again, horizontal motion directions were consistently associated with earlier saccadic inhibition times than vertical motion directions.

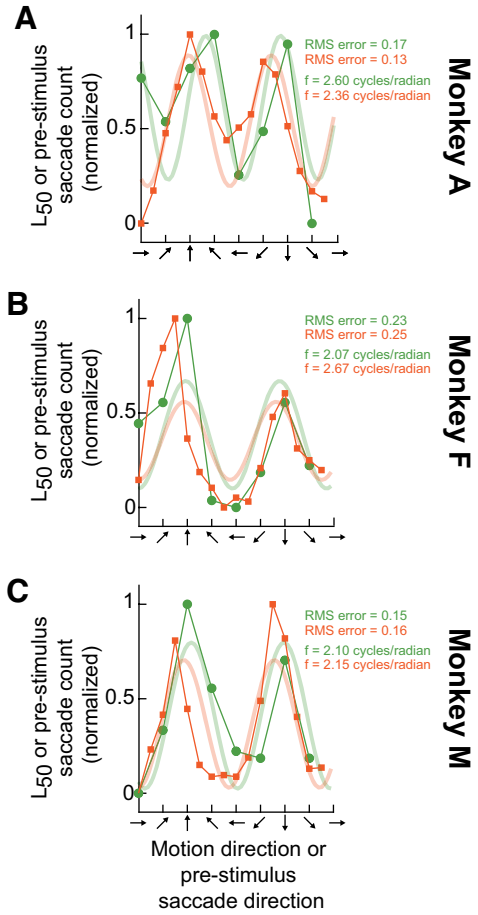

Figure 8. Similar directional anisotropies between saccadic inhibition and prestimulus baseline saccades (*experiment 6*). *A*: the green data points with connecting lines show saccadic inhibition time (L_{50}) measures from *monkey A* as a function of motion direction (these are the same data as in Fig. 7*B* with the only difference being that we normalized the dynamic range of the measurements to the interval between 0 and 1). The faint green continuous curve shows the best-fitting sinusoidal function to the same data [MATERIALS AND METHODS; root mean square (RMS) error values of the fit are shown]. The red data points with connecting lines show the likelihood of prestimulus baseline saccades of a given direction, and the faint red continuous curve is the best-fitting sinusoid. As can be seen, both the frequency and phase of the modulations with direction were similar for both the L_{50} and prestimulus baseline saccade data, consistent with the observations of Fig. 7. *B*: similar results for *monkey F*. *C*: similar results for *monkey M*.

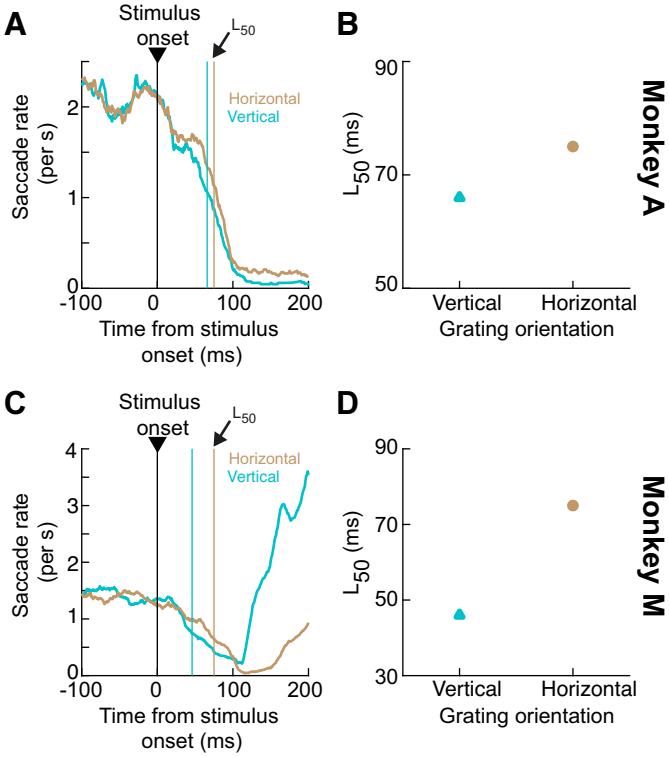

Figure 9. Later saccadic inhibition for horizontal gratings (*experiment 7*). *A*: raw saccade rate curves of *monkey A* from the 2 grating orientations tested in *experiment 7*. Each curve is truncated horizontally to focus on the saccadic inhibition phase. The vertical colored lines indicate saccadic inhibition time (L_{50}) for their respective saccade rate curves. As can be seen, saccadic inhibition occurred earlier for the vertical orientation than for the horizontal orientation. *B*: values of L_{50} in this experiment and animal for the 2 orientations. *C* and *D*: similar observations for *monkey M*.

Why would the oculomotor system need stronger and earlier saccadic inhibition for low spatial frequencies? One possibility is that low-spatial frequency stimuli are quite salient, and excitatory structures like the superior colliculus already favor these stimuli (56). Thus, because any spike in the superior colliculus can have an excitatory impact on the oculomotor system (62, 69), the inhibitory system that balances coordination with exogenous stimuli (3) would need to be equally potent for low-spatial frequency stimuli. A similar kind of logic also applies for stimulus contrast and size. Thus, we anticipate that circuits driving saccadic inhibition should have similar feature tuning preferences to circuits, such as the superior colliculus, that drive saccade generation.

We also find the motion direction effects on saccadic inhibition particularly intriguing. In all three animals, we found earlier saccadic inhibition, as evidenced by smaller L_{50} values, for horizontal than vertical motion directions. Although this observation is at least partially explained by grating orientation itself (Fig. 9), it remains interesting from the perspective of visual field asymmetries and oculomotor behavior, including in short-term memory (59, 70). In RESULTS, we also framed this anisotropy as potentially being related to the baseline anisotropies of saccade generation in the individual animals (Fig. 8). However, these explanations may not necessarily be mutually exclusive. For example, it could be that individual saccade directions are more or less likely in one animal exactly because of the animal's specific instantiation of visual field anisotropies in neural circuits. Indeed, given that saccades during fixation of a target (as in our experiments) primarily correct eye position errors even in explicit cuing tasks (30), the biased distributions of saccades in individual animals might reflect biased distributions of drift eye movements in the animals. Such drift eye movements, and the related saccades that intersperse them, continually expose the visual system to specific patterns of retinal image motion. They could thus either reflect or shape individual visual representational anisotropies in a given animal. It would be interesting in the future to relate saccadic inhibition properties to explicit experimentally controlled retinal image drifts.

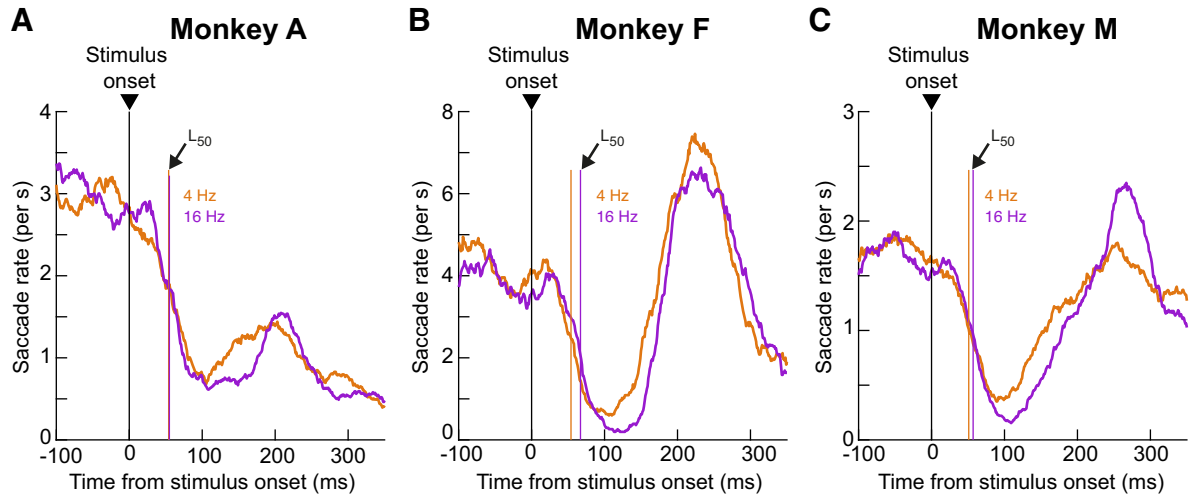

Figure 10. Longer-lasting saccadic inhibition for faster motions (*experiment 6*). *A*: *monkey A*. *B*: *monkey F*. *C*: *monkey M*. For each monkey, we collapsed across all motion directions from *experiment 6*, and we plotted the raw saccade rate curves. Saccadic inhibition timing (L_{50}, vertical colored lines) was generally similar for different motion speeds (caused by the different temporal frequencies of the drifting gratings). However, in all cases, the faster speed was associated with a longer-lasting saccadic inhibition period before the subsequent postinhibition saccades.

The above ideas fit well with the notion that the oculomotor system might implement its own "saliency model" based on features in the environment (71–75). Such a model might emphasize what is relevant for looking behavior per se (by eye movements), which might, in turn, be qualitatively different from what is needed for perceptual processing (33, 68). In that regard, it would be interesting in the future to consider how other features, such as color, might be relevant for saccadic inhibition.

In our stimulus contrast experiments, we also investigated the case in which a small stimulus was more like a distractor, or whether it became behaviorally relevant by requiring its foveation after saccadic inhibition was completed. We found that saccade rate dropped down to zero in the latter case. This makes functional sense. Every saccade is a bottleneck, and no other saccade can be generated at the same time. Therefore, for the target to be foveated saccade rate had to drop to zero. However, postinhibition saccades in the distractor case are also a bottleneck (because only 1 eye movement can be made at a time), and it is interesting to contemplate why saccadic inhibition was weaker in this case. One possibility is that there were two simultaneous sensory transients in the foveating condition: in addition to the stimulus onset, the fixation spot was removed at the same time to instruct the animals about the behavioral relevance of the appearing stimulus (and that it should be foveated). Therefore, it could be that there was a larger sensory drive for the inhibitory circuits. Interestingly, this larger sensory drive included input from both central (fixation spot removal) and peripheral (stimulus onset) visual representations. Given that our central presentation experiments, such as in Figs. 2–4, generally had significantly stronger saccadic inhibition effects than the peripheral experiments of Fig. 5, this suggests that saccadic inhibition strength could be sensitive to whether stimulus onsets occur in the fovea or not.

It would also be interesting in the future to study additional top-down impacts (like those potentially revealed by Fig. 5) on saccadic inhibition, but from a neurophysiological perspective. Such a perspective would exploit the use of monkeys as a model system for the phenomenon. For example, a variety of behavioral evidence in both humans and monkeys has shown interactions between saccade generation and saccadic inhibition, with pro- versus antisaccade instructions also significantly affecting microsaccade rates before and around stimulus onsets (5, 76–79). This likely serves a good function. For example, microsaccades near stimulus onset introduce a significant cost to perception and saccadic reaction times (5, 57, 80, 81). Therefore, if a task requires quick orienting responses, it makes sense to reduce prestimulus microsaccade rate (3) as we saw in Fig. 6. Other evidence of top-down influences on saccadic inhibition also includes modulations in inhibition strength by attention in instructed tasks (82) as well as by the type of text being read by subjects (51).

In terms of spatial context, the spatial alignment between stimulus onset and saccade goal location additionally matters in behavioral experiments with large saccades. Specifically, a task-irrelevant stimulus presented at the saccade goal location causes stronger saccadic inhibition (for large saccades) than the same stimulus presented remotely (8). These observations point toward an interaction between both temporal and spatial factors mediating coordination of external sensory events with internal movement programs (3, 69). Such factors can also easily apply to the case of microsaccades, which exhibit similar direction modulations with and without subsequent orienting responses (30).

Finally, several of our experiments included large stimulus onsets (e.g., full-screen flashes). We recently found that such onsets are associated with a stimulus-driven tiny drift of eye position (much smaller than microsaccades) (46). Such a drift response seems to also be stimulus driven.

However, the detailed feature tuning properties of this response, like in the case of saccadic inhibition, are still not fully explored. Given that the drift response seems to be coordinated with the time of saccadic inhibition, our goal in the near future is to document the feature tuning properties of the drift response in more detail, like we did here for saccadic inhibition. In this way, we would have a rich behavioral characterization of oculomotor phenomena related to the coordination between internal active perceptual state and asynchronous exogenous stimuli. Such characterization should open the door for interesting new insights about the underlying brain mechanisms of active perception and cognition.

APPENDIX

In this appendix, we include descriptive statistics of all saccadic inhibition measures that we obtained from all experiments and all animals individually. We also include measures of baseline saccade rate in the different experiments, as well as the total number of analyzed trials per experimental condition. The main numbers in Table A1 reflect the plotted results in all figures of this study, and Table A1 also includes estimates of 95% confidence intervals (within parentheses) obtained via 1,000 bootstraps (MATERIALS AND METHODS).

DATA AVAILABILITY

Table A1 in the APPENDIX lists all relevant summary statistics. Raw data will be made available upon request.

GRANTS

We were funded by the following grants from the Deutsche Forschungsgemeinschaft (DFG; German Research Foundation): BU4031/1-1, HA6749/4-1, BO5681/1-1, HA6749/3-1, and SFB 1233, Robust Vision: Inference Principles and Neural Mechanisms, TP11, project number: 276693517.

DISCLOSURES

No conflicts of interest, financial or otherwise, are declared by the authors.

AUTHOR CONTRIBUTIONS

Z.M.H. conceived and designed research; F.K., T.Z., M.P.B., A.B., T.M., Y.Y., and Z.M.H. performed experiments; F.K., T.Z., M.P.B., and Z.M.H. analyzed data; F.K., T.M., and Z.M.H. interpreted results of experiments; F.K. and Z.M.H. prepared figures; F.K. and Z.M.H. drafted manuscript; F.K. and Z.M.H.

Table A1. *Numerical measurements included in this study*

Animal	Baseline Saccade Rate (95% confidence interval), saccades/s	Condition	L_{50} (95% confidence interval), ms	R_{50} (95% confidence interval), saccades/s	Number of Trials
		Experiment 1: Size tuning			
A	2.00 (1.90, 2.17)	0.09°	54 (47, 63)	1.43 (1.26, 1.63)	1,371
		0.18°	60 (45, 66)	1.27 (1.09, 1.49)	1,344
		0.36°	56 (51, 62)	1.08 (0.92, 1.21)	1,388
		0.72°	55 (43, 60)	1.10 (0.10, 1.25)	1,402
		1.14°	47 (40, 53)	1.25 (1.15, 1.45)	1,341
		2.28°	48 (38, 57)	1.14 (1.07, 1.23)	1,447
		4.56°	49 (43, 57)	1.04 (0.87, 1.17)	1,369
		9.12°	50 (44, 55)	1.02 (0.89, 1.07)	1,394
F	3.49 (3.35, 3.64)	0.09°	75 (67, 80)	2.17 (2.06, 2.41)	1,033
		0.18°	65 (62, 71)	1.98 (1.76, 2.11)	999
		0.36°	55 (50, 60)	1.96 (1.78, 2.04)	1,017
		0.72°	61 (59, 65)	1.77 (1.68, 1.91)	1,044
		1.14°	55 (51, 58)	1.76 (1.56, 1.95)	1,093
		2.28°	49 (42, 50)	1.81 (1.69, 1.94)	1,089
		4.56°	45 (43, 47)	1.90 (1.76, 1.97)	1,003
		9.12°	43 (38, 44)	1.83 (1.74, 1.97)	1,068
M	1.90 (1.74, 2.06)	0.09°	76 (66, 99)	1.21 (0.99, 1.24)	628
		0.18°	59 (32, 68)	1.08 (0.92, 1,60)	655
		0.36°	54 (45, 61)	0.94 (0.78, 1.09)	661
		0.72°	42 (29, 47)	1.01 (0.91, 1.12)	710
		1.14°	40 (31, 46)	0.86 (0.72, 0.98)	713
		2.28°	50 (41, 57)	0.91 (0.81, 1.06)	660
		4.56°	44 (36, 51)	1.01 (0.89, 1.08)	664
		9.12°	39 (25, 48)	0.93 (0.80, 1.40)	632
		Experiment 2: Spatial frequency			
A	2.62 (2.42, 2.83)	0.5 cpd	55 (41, 67)	1.93 (1.51, 2.15)	483
		1 cpd	56 (42, 69)	1.66 (1.33, 1.89)	484
		2 cpd	64 (49, 74)	1.80 (1.45, 2.08)	484
		4 cpd	68 (39, 91)	2.05 (1.59, 2.26)	487
		8 cpd	83 (63, 95)	1.75 (1.46, 2.05)	484
F	3.60 (3.36, 3.85)	0.5 cpd	61 (48, 66)	1.84 (1.61, 2.26)	385
		1 cpd	62 (53, 70)	2.14 (1.87, 2.42)	389
		2 cpd	58 (39, 71)	2.45 (2.05, 2.82)	380
		4 cpd	81 (56, 89)	2.32 (2.06, 2.75)	385
		8 cpd	75 (62, 88)	2.46 (1.98, 2.71)	383

Continued

Table A1.— *Continued*

Animal	Baseline Saccade Rate (95% confidence interval), saccades/s	Condition	L_{50} (95% confidence interval), ms	R_{50} (95% confidence interval), saccades/s	Number of Trials
		Experiment 3: Contrast (full screen)			
A	2.34 (2.22, 2.46)	5%	75 (65, 86)	1.62 (1.39, 1.76)	1,315
		10%	68 (61, 77)	1.49 (1.27, 1.63)	1,308
		20%	52 (43, 62)	1.51 (1.26, 1.61)	1,315
		40%	58 (50, 66)	1.30 (1.13, 1.44)	1,321
		80%	54 (45, 60)	1.31 (1.12, 1.45)	1,321
F	3.58 (3.40, 3.75)	5%	69 (58, 75)	2.20 (1.92, 2.44)	767
		10%	49 (37, 58)	2.15 (1.84, 2.38)	771
		20%	52 (45, 59)	2.11 (1.90, 2.30)	766
		40%	53 (47, 59)	1.93 (1.69, 2.16)	776
		80%	43 (36, 50)	1.84 (1.62, 2.03)	760
M	1.94 (1.8, 2.09)	5%	57 (46, 104)	1.37 (1.15, 1.55)	785
		10%	69 (55, 99)	1.23 (0.96, 1.53)	789
		20%	51 (34, 61)	1.21 (1.00, 1.39)	790
		40%	43 (30, 63)	1.25 (0.93, 1.38)	785
		80%	41 (32, 49)	1.14 (0.95, 1.28)	788
		Experiment 4: Contrast (small stimulus)			
A	2.15 (1.98, 2.32)	5%	60 (44, 102)	1.64 (1.32, 1.87)	627
		10%	80 (54, 90)	1.24 (1.03, 1.52)	623
		20%	63 (47, 77)	1.44 (1.16, 1.61)	622
		50%	57 (43, 68)	1.17 (0.95, 1.35)	626
		100%	42 (28, 58)	1.40 (1.06 1.57)	623
M	2.21 (2.10, 2.33)	5%	91 (71, 111)	1.49 (1.32, 1.66)	1,689
		10%	62 (41, 78)	1.33 (1.20, 1.50)	1,689
		20%	49 (32, 65)	1.54 (1.34, 1.65)	1,682
		50%	44 (29, 58)	1.49 (1.32, 1.60)	1,677
		100%	49 (39, 59)	1.47 (1.32, 1.61)	1,692
		Experiment 5: Contrast (foveating saccade)			
A	1.29 (1.14, 1.44)	10%	60 (43, 70)	0.60 (0.48, 0.88)	498
		20%	60 (40, 70)	0.64 (0.50, 0.87)	439
		50%	53 (35, 67)	0.72 (0.57, 0.91)	495
		100%	38 (20, 54)	0.64 (0.47, 0.83)	497
F	2.40 (2.25, 2.55)	5%	71 (62, 78)	1.39 (1.19 1.55)	915
		10%	72 (63, 78)	1.15 (1.00, 1.32)	878
		50%	59 (52, 66)	1.32 (1.17, 1.48)	888
		100%	58 (49, 66)	1.13 (0.97, 1.37)	883
M	1.51 (1.38, 1.64)	5%	66 (44, 69)	1.15 (0.43, 1.92)	52
		10%	61 (51, 68)	0.79 (0.64, 0.93)	805
		50%	56 (49, 65)	0.88 (0.70, 1.01)	808
		100%	62 (54, 69)	0.82 (0.61, 0.93)	806
		Experiment 6: Motion direction (pooled across temporal frequencies)			
A	2.78 (2.57, 2.98)	Up	63 (48, 80)	2.00 (1.58, 2.26)	479
		Up-right	52 (37, 73)	1.57 (1.18, 1.80)	479
		Right	61 (52, 73)	1.81 (1.45, 2.03)	486
		Down-right	31 (19, 53)	2.24 (1.74, 2.37)	482
		Down	68 (49, 79)	1.64 (1.33, 1.92)	480
		Down-left	50 (37, 63)	1.66 (1.36, 1.91)	484
		Left	41 (21, 59)	2.09 (1.71, 2.36)	479
		Up-left	70 (56, 84)	1.80 (1.42, 2.04)	486
F	4.37 (3.96, 4.77)	Up	79 (52, 100)	1.64 (1.37, 2.48)	157
		Up-right	67 (44, 77)	2.23 (1.70, 2.82)	154
		Right	64 (48, 76)	2.48 (1.75, 2.82)	150
		Down-right	58 (44, 70)	2.11 (1.58, 2.56)	154
		Down	67 (51, 80)	2.01 (1.45, 2.60)	148
		Down-left	57 (32, 77)	2.40 (1.88, 2.88)	153
		Left	52 (33, 69)	2.70 (1.90, 2.98)	151
		Up-left	53 (29, 67)	2.24 (1.78, 2.90)	151
M	2.0 (1.84, 2.15)	Up	64 (44, 73)	0.92 (0.78, 1.16)	737
		Up-right	46 (25, 58)	0.98 (0.81, 1.19)	732
		Right	37 (26, 50)	0.99 (0.73, 1.12)	745
		Down-right	42 (25, 56)	0.97 (0.78, 1.11)	745
		Down	56 (40, 68)	1.07 (0.84, 1.25)	752
		Down-left	42 (30, 54)	0.95 (0.75, 1.14)	753
		Left	43 (33, 54)	1.01 (0.81, 1.20)	756
		Up-left	52 (39, 59)	1.03 (0.86, 1.24)	741

Continued

Table A1.— *Continued*

Animal	Baseline Saccade Rate (95% confidence interval), saccades/s	Condition	L_{50} (95% confidence interval), ms	R_{50} (95% confidence interval), saccades/s	Number of Trials
		Experiment 7: Orientation tuning			
A	2.12 (1.92, 2.31)	Horizontal	75 (58, 83)	1.15 (1.02, 1.30)	1,352
		Vertical	66 (48, 74)	1.08 (0.96, 1.23)	1,338
M	1.41 (1.28, 1.54)	Horizontal	75 (56, 83)	0.69 (0.63, 0.82)	2,457
		Vertical	46 (35, 56)	0.79 (0.70, 0.90)	2,458

Baseline saccade rate was obtained from the final 100 ms of fixation before stimulus onset. MATERIALS AND METHODS describes how saccadic inhibition time (L_{50}) and strength (R_{50}) were obtained.

edited and revised manuscript; F.K., T.Z., M.P.B., A.B., T.M., Y.Y., and Z.M.H. approved final version of manuscript.

REFERENCES

1. **Reingold EM**, **Stampe DM.** Saccadic inhibition in complex visual tasks. In: *Current Oculomotor Research*, edited by Becker W, Deubel H, Mergner T. Boston, MA: Springer, 1999, p. 249–255.
2. **Reingold EM**, **Stampe DM.** Saccadic inhibition in voluntary and reflexive saccades. *J Cogn Neurosci* 14: 371–388, 2002. doi:10.1162/089892902317361903.
3. **Buonocore A**, **Hafed ZM.** The inevitability of visual interruption. *J Neurophysiol* 130: 225–237, 2023., doi:10.1152/jn.00441.2022.
4. **Engbert R**, **Kliegl R.** Microsaccades uncover the orientation of covert attention. *Vision Res* 43: 1035–1045, 2003. doi:10.1016/s0042-6989(03)00084-1.
5. **Hafed ZM**, **Lovejoy LP**, **Krauzlis RJ.** Modulation of microsaccades in monkey during a covert visual attention task. *J Neurosci* 31: 15219–15230, 2011. doi:10.1523/JNEUROSCI.3106-11.2011.
6. **Buonocore A**, **McIntosh RD.** Saccadic inhibition underlies the remote distractor effect. *Exp Brain Res* 191: 117–122, 2008. doi:10.1007/s00221-008-1558-7.
7. **Edelman JA**, **Xu KZ.** Inhibition of voluntary saccadic eye movement commands by abrupt visual onsets. *J Neurophysiol* 101: 1222–1234, 2009. doi:10.1152/jn.90708.2008.
8. **Buonocore A**, **McIntosh RD.** Modulation of saccadic inhibition by distractor size and location. *Vision Res* 69: 32–41, 2012. doi:10.1016/j.visres.2012.07.010.
9. **Bompas A**, **Sumner P**, **Hedge C.** Non-decision time: the Higg's boson of decision (Preprint). *BioRxiv* 2023.02.20.529290, 2023. doi:10.1101/2023.02.20.529290.
10. **Scholes C**, **McGraw PV**, **Nyström M**, **Roach NW.** Fixational eye movements predict visual sensitivity. *Proc Biol Sci* 282: 20151568, 2015. doi:10.1098/rspb.2015.1568.
11. **Bonneh YS**, **Adini Y**, **Polat U.** Contrast sensitivity revealed by microsaccades. *J Vis* 15: 11, 2015. doi:10.1167/15.9.11.
12. **Rolfs M**, **Kliegl R**, **Engbert R.** Toward a model of microsaccade generation: the case of microsaccadic inhibition. *J Vis* 8: 5 1–23, 2008. doi:10.1167/8.11.5.
13. **Buonocore A**, **Skinner J**, **Hafed ZM.** Eye position error influence over "open-loop" smooth pursuit initiation. *J Neurosci* 39: 2709–2721, 2019. doi:10.1523/JNEUROSCI.2178-18.2019.
14. **Kerzel D**, **Born S**, **Souto D.** Inhibition of steady-state smooth pursuit and catch-up saccades by abrupt visual and auditory onsets. *J Neurophysiol* 104: 2573–2585, 2010. doi:10.1152/jn.00193.2010.
15. **Stolte M**, **Kraus L**, **Ansorge U.** Visual attentional guidance during smooth pursuit eye movements: distractor interference is independent of distractor-target similarity. *Psychophysiology* 2023: e14384, 2023. doi:10.1111/psyp.14384.
16. **Ziv I**, **Bonneh YS.** Oculomotor inhibition during smooth pursuit and its dependence on contrast sensitivity. *J Vis* 21: 12, 2021. doi:10.1167/jov.21.2.12.
17. **Xue L**, **Huang D**, **Wang T**, **Hu Q**, **Chai X**, **Li L**, **Chen Y.** Dynamic modulation of the perceptual load on microsaccades during a selective spatial attention task. *Sci Rep* 7: 16496, 2017. doi:10.1038/s41598-017-16629-2.
18. **Yu G**, **Herman JP**, **Katz LN**, **Krauzlis RJ.** Microsaccades as a marker not a cause for attention-related modulation. *eLife* 11: e74168, 2022. doi:10.7554/eLife.74168.
19. **Buonocore A**, **Chen CY**, **Tian X**, **Idrees S**, **Münch TA**, **Hafed ZM.** Alteration of the microsaccadic velocity-amplitude main sequence relationship after visual transients: implications for models of saccade control. *J Neurophysiol* 117: 1894–1910, 2017. doi:10.1152/jn.00811.2016.
20. **Orczyk JJ**, **Barczak A**, **O'Connell MN**, **Kajikawa Y.** Saccadic inhibition during free viewing in macaque monkeys. *J Neurophysiol* 129: 356–367, 2023. doi:10.1152/jn.00225.2022.
21. **Hafed ZM**, **Yoshida M**, **Tian X**, **Buonocore A**, **Malevich T.** Dissociable cortical and subcortical mechanisms for mediating the influences of visual cues on microsaccadic eye movements. *Front Neural Circuits* 15: 638429, 2021. doi:10.3389/fncir.2021.638429.
22. **Salinas E**, **Stanford TR.** Saccadic inhibition interrupts ongoing oculomotor activity to enable the rapid deployment of alternate movement plans. *Sci Rep* 8: 14163, 2018. doi:10.1038/s41598-018-32224-5.
23. **Bompas A**, **Sumner P.** Saccadic inhibition reveals the timing of automatic and voluntary signals in the human brain. *J Neurosci* 31: 12501–12512, 2011. doi:10.1523/JNEUROSCI.2234-11.2011.
24. **Bompas A**, **Campbell AE**, **Sumner P.** Cognitive control and automatic interference in mind and brain: a unified model of saccadic inhibition and countermanding. *Psychol Rev* 127: 524–561, 2020. doi:10.1037/rev0000181.
25. **Trappenberg TP**, **Dorris MC**, **Munoz DP**, **Klein RM.** A model of saccade initiation based on the competitive integration of exogenous and endogenous signals in the superior colliculus. *J Cogn Neurosci* 13: 256–271, 2001. doi:10.1162/089892901564306.
26. **Hafed ZM**, **Lovejoy LP**, **Krauzlis RJ.** Superior colliculus inactivation alters the relationship between covert visual attention and microsaccades. *Eur J Neurosci* 37: 1169–1181, 2013. doi:10.1111/ejn.12127.
27. **Peel TR**, **Hafed ZM**, **Dash S**, **Lomber SG**, **Corneil BD.** A causal role for the cortical frontal eye fields in microsaccade deployment. *PLoS Biol* 14: e1002531, 2016. doi:10.1371/journal.pbio.1002531.
28. **Malevich T**, **Buonocore A**, **Hafed ZM.** Dependence of the stimulus-driven microsaccade rate signature in rhesus macaque monkeys on visual stimulus size and polarity. *J Neurophysiol* 125: 282–295, 2021. doi:10.1152/jn.00304.2020.
29. **Tian X**, **Yoshida M**, **Hafed ZM.** Dynamics of fixational eye position and microsaccades during spatial cueing: the case of express microsaccades. *J Neurophysiol* 119: 1962–1980, 2018. doi:10.1152/jn.00752.2017.
30. **Tian X**, **Yoshida M**, **Hafed ZM.** A microsaccadic account of attentional capture and inhibition of return in Posner cueing. *Front Syst Neurosci* 10: 23, 2016. doi:10.3389/fnsys.2016.00023.
31. **Hafed ZM**, **Chen CY**, **Tian X**, **Baumann M**, **Zhang T.** Active vision at the foveal scale in the primate superior colliculus. *J Neurophysiol* 125: 1121–1138, 2021., doi:10.1152/jn.00724.2020.
32. **Otero-Millan J**, **Macknik SL**, **Langston RE**, **Martinez-Conde S.** An oculomotor continuum from exploration to fixation. *Proc Natl Acad Sci USA* 110: 6175–6180, 2013. doi:10.1073/pnas.1222715110.
33. **Hafed ZM**, **Hoffmann KP**, **Chen CY**, **Bogadhi AR.** Visual functions of the primate superior colliculus. *Annu Rev Vis Sci* 9: 361–383, 2023. doi:10.1146/annurev-vision-111022-123817.
34. **Malevich T**, **Zhang T**, **Baumann MP**, **Bogadhi AR**, **Hafed ZM.** Faster detection of "darks" than "brights" by monkey superior colliculus

neurons. *J Neurosci* 42: 9356–9371, 2022. doi:10.1523/JNEUROSCI.1489-22.2022.
35. **Bogadhi AR**, **Buonocore A**, **Hafed ZM.** Task-irrelevant visual forms facilitate covert and overt spatial selection. *J Neurosci* 40: 9496–9506, 2020. doi:10.1523/JNEUROSCI.1593-20.2020.
36. **Bogadhi AR**, **Hafed ZM.** Express detection and discrimination of visual objects by primate superior colliculus neurons (Preprint). *BioRxiv* 2022.02.08.479583, 2022. doi:10.1101/2022.02.08.479583.
37. **Eastman KM**, **Huk AC.** PLDAPS: a hardware architecture and software toolbox for neurophysiology requiring complex visual stimuli and online behavioral control. *Front Neuroinform* 6: 1, 2012. doi:10.3389/fninf.2012.00001.
38. **Brainard DH.** The Psychophysics Toolbox. *Spat Vis* 10: 433–436, 1997.
39. **Pelli DG.** The VideoToolbox software for visual psychophysics: transforming numbers into movies. *Spat Vis* 10: 437–442, 1997.
40. **Kleiner M**, **Brainard D**, **Dg P.** What's new in Psychtoolbox-3? (Abstract). *Perception* 36: 14, 2007.
41. **Baumann MP**, **Bogadhi AR**, **Denninger AF**, **Hafed ZM.** Sensory tuning in neuronal movement commands. *Proc Natl Acad Sci USA* 120: e2305759120, 2023. doi:10.1073/pnas.2305759120.
42. **Fuchs AF**, **Robinson DA.** A method for measuring horizontal and vertical eye movement chronically in the monkey. *J Appl Physiol* 21: 1068–1070, 1966. doi:10.1152/jappl.1966.21.3.1068.
43. **Judge SJ**, **Richmond BJ**, **Chu FC.** Implantation of magnetic search coils for measurement of eye position: an improved method. *Vision Res* 20: 535–538, 1980. doi:10.1016/0042-6989(80)90128-5.
44. **Laubrock J**, **Engbert R**, **Kliegl R.** Fixational eye movements predict the perceived direction of ambiguous apparent motion. *J Vis* 8: 13, 2008. doi:10.1167/8.14.13.
45. **Yeh CI**, **Xing D**, **Shapley RM.** "Black" responses dominate macaque primary visual cortex V1. *J Neurosci* 29: 11753–11760, 2009. doi:10.1523/JNEUROSCI.1991-09.2009.
46. **Malevich T**, **Buonocore A**, **Hafed ZM.** Rapid stimulus-driven modulation of slow ocular position drifts. *eLife* 9: e57595, 2020. doi:10.7554/eLife.57595.
47. **Chen CY**, **Hafed ZM.** Postmicrosaccadic enhancement of slow eye movements. *J Neurosci* 33: 5375–5386, 2013. doi:10.1523/JNEUROSCI.3703-12.2013.
48. **Bellet ME**, **Bellet J**, **Nienborg H**, **Hafed ZM**, **Berens P.** Human-level saccade detection performance using deep neural networks. *J Neurophysiol* 121: 646–661, 2019. doi:10.1152/jn.00601.2018.
49. **Gandhi NJ**, **Bonadonna DK.** Temporal interactions of air-puff-evoked blinks and saccadic eye movements: insights into motor preparation. *J Neurophysiol* 93: 1718–1729, 2005. doi:10.1152/jn.00854.2004.
50. **Collewijn H**, **van der Steen J**, **Steinman RM.** Human eye movements associated with blinks and prolonged eyelid closure. *J Neurophysiol* 54: 11–27, 1985. doi:10.1152/jn.1985.54.1.11.
51. **Reingold EM**, **Stampe DM.** Saccadic inhibition in reading. *J Exp Psychol Hum Percept Perform* 30: 194–211, 2004. doi:10.1037/0096-1523.30.1.194.
52. **Hafed ZM**, **Ignashchenkova A.** On the dissociation between microsaccade rate and direction after peripheral cues: microsaccadic inhibition revisited. *J Neurosci* 33: 16220–16235, 2013. doi:10.1523/JNEUROSCI.2240-13.2013.
53. **Hsu TY**, **Chen JT**, **Tseng P**, **Wang CA.** Role of the frontal eye field in human microsaccade responses: a TMS study. *Biol Psychol* 165: 108202, 2021. doi:10.1016/j.biopsycho.2021.108202.
54. **Barquero C**, **Chen JT**, **Munoz DP**, **Wang CA.** Human microsaccade cueing modulation in visual- and memory-delay saccade tasks after theta burst transcranial magnetic stimulation over the frontal eye field. *Neuropsychologia* 187: 108626, 2023. doi:10.1016/j.neuropsychologia.2023.108626.
55. **Buonocore A**, **Purokayastha S**, **McIntosh RD.** Saccade reorienting is facilitated by pausing the oculomotor program. *J Cogn Neurosci* 29: 2068–2080, 2017. doi:10.1162/jocn_a_01179.
56. **Chen CY**, **Sonnenberg L**, **Weller S**, **Witschel T**, **Hafed ZM.** Spatial frequency sensitivity in macaque midbrain. *Nat Commun* 9: 2852, 2018. doi:10.1038/s41467-018-05302-5.
57. **Chen CY**, **Hafed ZM.** A neural locus for spatial-frequency specific saccadic suppression in visual-motor neurons of the primate superior colliculus. *J Neurophysiol* 117: 1657–1673, 2017. doi:10.1152/jn.00911.2016.
58. **Hafed ZM**, **Clark JJ.** Microsaccades as an overt measure of covert attention shifts. *Vision Res* 42: 2533–2545, 2002. doi:10.1016/s0042-6989(02)00263-8.
59. **Carrasco M**, **Talgar CP**, **Cameron EL.** Characterizing visual performance fields: effects of transient covert attention, spatial frequency, eccentricity, task and set size. *Spat Vis* 15: 61–75, 2001. doi:10.1163/15685680152692015.
60. **Talgar CP**, **Carrasco M.** Vertical meridian asymmetry in spatial resolution: visual and attentional factors. *Psychon Bull Rev* 9: 714–722, 2002. doi:10.3758/bf03196326.
61. **Liu T**, **Heeger DJ**, **Carrasco M.** Neural correlates of the visual vertical meridian asymmetry. *J Vis* 6: 1294–1306, 2006. doi:10.1167/6.11.12.
62. **Edelman JA**, **Keller EL.** Activity of visuomotor burst neurons in the superior colliculus accompanying express saccades. *J Neurophysiol* 76: 908–926, 1996. doi:10.1152/jn.1996.76.2.908.
63. **Keller EL.** Participation of medial pontine reticular formation in eye movement generation in monkey. *J Neurophysiol* 37: 316–332, 1974. doi:10.1152/jn.1974.37.2.316.
64. **Missal M**, **Keller EL.** Common inhibitory mechanism for saccades and smooth-pursuit eye movements. *J Neurophysiol* 88: 1880–1892, 2002. doi:10.1152/jn.2002.88.4.1880.
65. **Everling S**, **Paré M**, **Dorris MC**, **Munoz DP.** Comparison of the discharge characteristics of brain stem omnipause neurons and superior colliculus fixation neurons in monkey: implications for control of fixation and saccade behavior. *J Neurophysiol* 79: 511–528, 1998. doi:10.1152/jn.1998.79.2.511.
66. **Hafed ZM**, **Chen CY.** Sharper, stronger, faster upper visual field representation in primate superior colliculus. *Curr Biol* 26: 1647–1658, 2016. doi:10.1016/j.cub.2016.04.059.
67. **Fracasso A**, **Buonocore A**, **Hafed ZM.** Peri-saccadic orientation identification performance and visual neural sensitivity are higher in the upper visual field. *J Neurosci* 43: 6884–6897, 2023. doi:10.1523/JNEUROSCI.1740-22.2023.
68. **Previc FH.** Functional specialization in the lower and upper visual-fields in humans—its ecological origins and neurophysiological implications. *Behav Brain Sci* 13: 519–542, 1990. doi:10.1017/S0140525X00080018.
69. **Buonocore A**, **Tian X**, **Khademi F**, **Hafed ZM.** Instantaneous movement-unrelated midbrain activity modifies ongoing eye movements. *eLife* 10: e64150, 2021. doi:10.7554/eLife.64150.
70. **Willeke KF**, **Cardenas AR**, **Bellet J**, **Hafed ZM.** Severe distortion in the representation of foveal visual image locations in short-term memory. *Proc Natl Acad Sci USA* 119: e2121860119, 2022. doi:10.1073/pnas.2121860119.
71. **Yoshida M**, **Itti L**, **Berg DJ**, **Ikeda T**, **Kato R**, **Takaura K**, **White BJ**, **Munoz DP**, **Isa T.** Residual attention guidance in blindsight monkeys watching complex natural scenes. *Curr Biol* 22: 1429–1434, 2012. doi:10.1016/j.cub.2012.05.046.
72. **White BJ**, **Berg DJ**, **Kan JY**, **Marino RA**, **Itti L**, **Munoz DP.** Superior colliculus neurons encode a visual saliency map during free viewing of natural dynamic video. *Nat Commun* 8: 14263, 2017. doi:10.1038/ncomms14263.
73. **White BJ**, **Kan JY**, **Levy R**, **Itti L**, **Munoz DP.** Superior colliculus encodes visual saliency before the primary visual cortex. *Proc Natl Acad Sci USA* 114: 9451–9456, 2017. doi:10.1073/pnas.1701003114.
74. **Veale R**, **Hafed ZM**, **Yoshida M.** How is visual salience computed in the brain? Insights from behaviour, neurobiology and modelling. *Philos Trans R Soc Lond B Biol Sci* 372: 20160113, 2017. doi:10.1098/rstb.2016.0113.
75. **Kümmerer M**, **Bethge M.** Predicting visual fixations. *Annu Rev Vis Sci* 9: 269–291, 2023. doi:10.1146/annurev-vision-120822-072528.
76. **Yu G**, **Xu B**, **Zhao Y**, **Zhang B**, **Yang M**, **Kan JY**, **Milstein DM**, **Thevarajah D**, **Dorris MC.** Microsaccade direction reflects the economic value of potential saccade goals and predicts saccade choice. *J Neurophysiol* 115: 741–751, 2016. doi:10.1152/jn.00987.2015.
77. **Watanabe M**, **Matsuo Y**, **Zha L**, **Munoz DP**, **Kobayashi Y.** Fixational saccades reflect volitional action preparation. *J Neurophysiol* 110: 522–535, 2013. doi:10.1152/jn.01096.2012.
78. **Krasovskaya S**, **Kristjánsson Á**, **MacInnes WJ.** Microsaccade rate activity during the preparation of pro- and antisaccades. *Atten Percept Psychophys* 85: 2257–2276, 2023. doi:10.3758/s13414-023-02731-3.

79. **Dalmaso M**, **Castelli L**, **Galfano G.** Microsaccadic rate and pupil size dynamics in pro-/anti-saccade preparation: the impact of intermixed vs. blocked trial administration. *Psychol Res* 84: 1320–1332, 2020. doi:10.1007/s00426-018-01141-7.
80. **Hafed ZM.** Alteration of visual perception prior to microsaccades. *Neuron* 77: 775–786, 2013. doi:10.1016/j.neuron.2012.12.014.
81. **Hafed ZM**, **Krauzlis RJ.** Microsaccadic suppression of visual bursts in the primate superior colliculus. *J Neurosci* 30: 9542–9547, 2010. doi:10.1523/JNEUROSCI.1137-10.2010.
82. **Buonocore A**, **McIntosh RD.** Attention modulates saccadic inhibition magnitude. *Q J Exp Psychol (Hove)* 66: 1051–1059, 2013. doi:10.1080/17470218.2013.797001.